S. Klevering

# Foot-operated tele-impedance control interface for robot manipulation tasks involving interaction with unstructured and unpredictable environments

## MSc Thesis

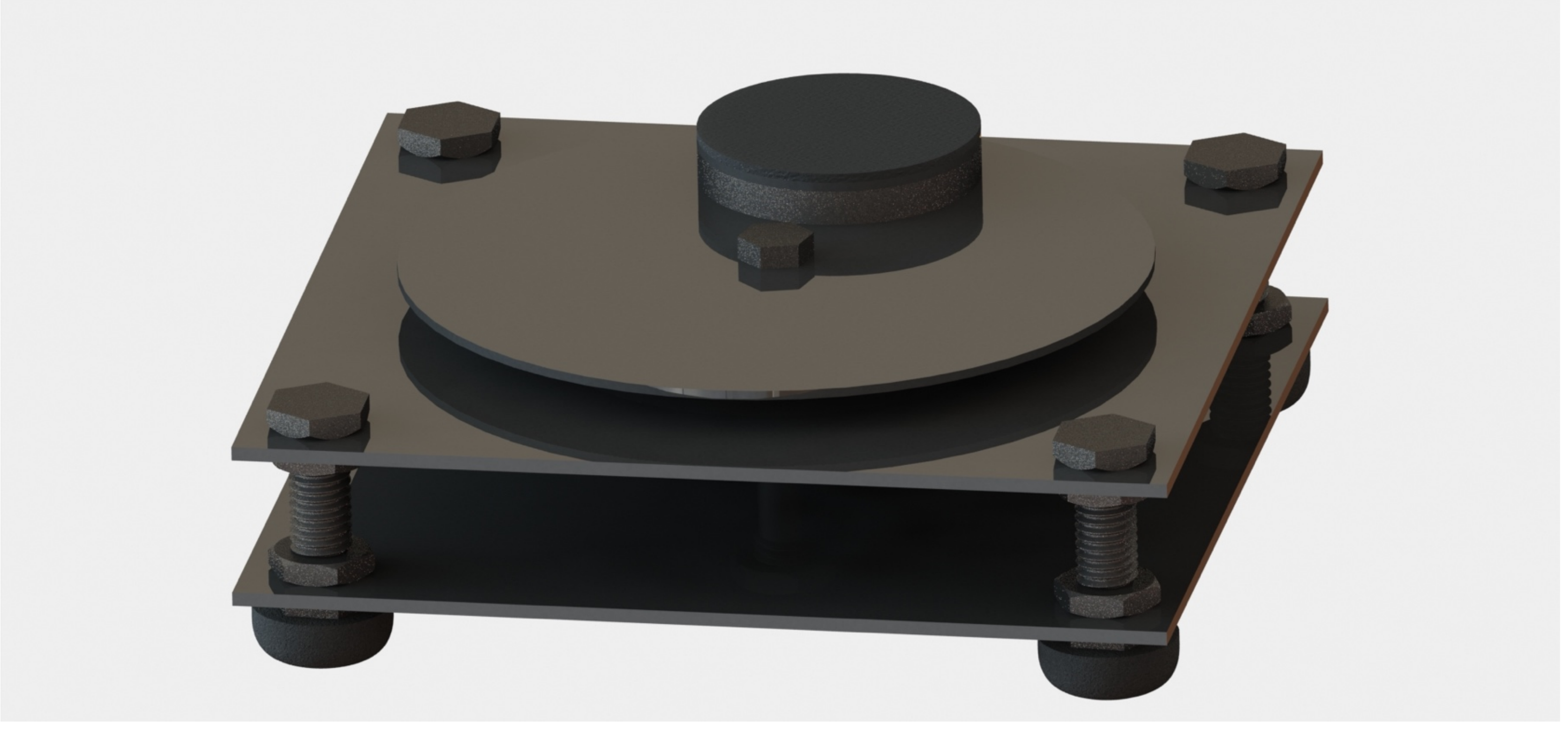

-

# Foot-operated tele-impedance control interface for robot manipulation tasks involving interaction with unstructured and unpredictable environments

## MSc Thesis

by

## S. Klevering

to obtain the degree of Master of Science
at the Delft University of Technology,
to be defended publicly on Tuesday March 31, 2021 at 10:00 AM.

| | | |
|---|---|---|
| Student number: | 4224329 | |
| Thesis committee: | Prof. dr. ir. D.A. Abbink, | Cognitive Robotics, Department of Mechanical Engineering, TU Delft, supervisor |
| | Dr. ir. W. Mugge, | Biomechatronics & Human-Machine Control, Department of Biomedical Engineering, TU Delft, supervisor |
| | Dr. L. Peternel, | Cognitive Robotics, Department of Mechanical Engineering, TU Delft, supervisor |
| | Dr. Ir. M.M. van Paassen, | Control & Operations, Department of Aerospace Engineering, TU Delft |

An electronic version of this thesis is available at `http://repository.tudelft.nl/`.

# Preface

During my MSc Thesis project, I first did a literature study about the implementation of tele-impedance in robotic surgical systems. I found out that most of the existing tele-impedance methods were specifically for one goal or application and not very practical. Especially evaluating tele-impedance control in robotic surgical systems resulted in many constraints. Therefore, I focused on a design of a interface which would be easy to implement in various applications.

The goal brought me to the design of the circular disc interface, which I created and manufactured at the TU Delft. The main objective of this research is to determine the performance of the circular disc interface interacting with an unpredictable and unstructured environment.

The first part of this report consists of a scientific journal paper summarizing the design of the circular disc interface and a human factors experiment. The human factors experiment was conducted to validate the design regarding interaction performance between tool and environment. Furthermore, analysis has been done on how the operator controls the circular stiffness ellipse. The second part consists of appendices to provide more insight of the experimental study as the interface design. This will allow future students or researchers to have access for more in-depth information of this project.

Appendix A describes the tele-impedance control architecture. Appendix B explains the circular disc interface. Appendix C the ideal stiffness ellipse strategy for the circular disc interface during a drilling task. Appendix D further describes the experiment methods and Appendix E gives more information about the experiment results.

I want to thank everyone who has contributed to the completion of my MSc project. In particular, I want to thank Luka Peternel, David Abbink and Winfred Mugge for the close supervision, guidance and advice for my thesis project.

*S. Klevering*
*Delft, March 2021*

# Contents

1 Scientific Paper 1

A Tele-impedance control architecture 13
  A.1 Assumptions 13
  A.2 Bilateral and Unilateral teleoperation 13
    A.2.1 Movement in free space 14
    A.2.2 Interaction with the wall 15
    A.2.3 Applied force perturbation 15

B Circular disc interface 17
  B.1 Design requirements 17
  B.2 Circular disc interface design 17
    B.2.1 Rotating disc 17
    B.2.2 foot pad 18
    B.2.3 sensors 19
  B.3 Technical Drawings and HREC device report 19

C Ideal stiffness ellipse strategy 27

D Experiment methods 29
  D.1 Experiment design 29
    D.1.1 Independent variables 29
    D.1.2 Drilling task 29
    D.1.3 Drill insertion 30
    D.1.4 Randomization of trials 31
    D.1.5 Perturbation design 31
  D.2 Matlab and C++ code 33
  D.3 Understanding and training 34
    D.3.1 Understanding session 34
  D.4 Informed Consent 35
  D.5 NASA TLX 38

E Experiment results 41
  E.1 Ideal stiffness ellipse strategy 41
  E.2 Stiffness ellipse semi-major axis elongation 42
  E.3 Rotational accuracy 43

Bibliography 45

# 1

# Scientific Paper

# Foot-operated tele-impedance control interface for robot manipulation tasks involving interaction with unstructured and unpredictable environments

Stijn Klevering
Supervised by:
Winfred Mugge, David A. Abbink, and Luka Peternel

*Abstract*—**Tele-impedance can increase interaction performance between a robotic tool and unstructured/unpredictable environment during teleoperation. However, the existing tele-impedance interfaces have several ongoing issues, such as long calibration times and various obstructions for the human operator. In addition, they are all designed to be controlled by the operator's arms, which can cause difficulties when both arms are used, as in bi-manual teleoperation. To resolve these issues, we designed novel foot-based tele-impedance control method inspired by the human limb stiffness ellipse modulation. The proposed mechanical interface is based around a circular disc and a foot pressure sensor that controls orientation and size/shape of the stiffness ellipsoid, respectively, by the operator's foot. We evaluated the circular disc interface control method in an experimental study with 12 participants, who performed a two-dimensional drilling task in a virtual environment. The results show the ability of the operator in controlling the proposed interface to dynamically adapt to task instruction and environment. In addition, a comparison with low and high constant impedance control demonstrate a superior interaction performance of the proposed interface.**

## I. INTRODUCTION

Teleoperation enables the operator to complete tasks at a distance by a robotic system over a communication network. The use of teleoperation systems are motivated by issues of human safety in hazardous environments, high cost of reaching remote environments and adaptation to scale [1]. It enables a range of applications across domains including deep-sea and space exploration, handling of hazardous materials, military, first responder, assembly and remote surgery. During execution of teleoperation tasks, the operator has to deal with unpredictable and unstructured environments due to position, force and visual disturbances causing poor performance and stability issues [2]. This is especially true for deep-sea remotely operated vehicles that have to deal with motion and visual disturbances by waves or turbid water, which are detrimental for successful task execution [3].

Successful task execution often demands extensive contact with the environment and typically consists of accurate force regulation and accurate end-effector position control objectives [4]. With purely position controlled manipulation, the most common type of manipulation, manipulators tend to lose contact or create high interaction forces with the environment, resulting in disastrous consequences regarding damaging the environment, manipulator or tool. Furthermore, as task difficulty increases, the task will become more time consuming or will even become impossible to complete successfully [3], [5]. The introduction of motion, force and visual disturbances will decrease the interaction performance between tool and environment and are therefore highly detrimental for successful task completion.

A solution to increase interaction performance between tool and environment presented is the inclusion of force feedback to convey proprioceptive or haptic feedback of the manipulator and interaction with the remote environment, which greatly increases telepresence but can be detrimental for stability in some cases [3], [4], [6], [7]. Another solution to increase interaction performance between tool and environment is a control architecture called tele-impedance [8]–[10].

Tele-impedance gives the operator the ability to dynamically change the impedance of the manipulator by replicating the behavior of human arm impedance strategies [10]. Characteristic applications are assembly, human-robot co-manipulation and exoskeletons [9], [11]–[13]. Human arm impedance strategies substantially depend on task instruction [14], [15].

The human decreases the impedance of the limb to accurately control reference forces during force tasks [14]. Position tasks increase human arm impedance to hold posture and increase accuracy during reaching tasks [16]. Consequently, tele-impedance results in increased position and force control while having the ability to compensate for unpredictable perturbations depending on task instruction [10], [17].

Nowadays, existing methods enabling tele-impedance can be divided in two main categories. The first category consists of electromyography-based (EMG) methods, which estimates the stiffness of the operator arm by muscle activation and posture estimation [12], [18]–[20]. Generally, the force and impedance of the operator are estimated by using musculoskeletal models including the inputs of agonist and antagonist EMG measurements and position measurements of the operators arm [10], [21]. EMG-based methods have the ability to generate multi-dimensional variable impedance but generally create an obstruction for the operator due to long calibration times and additional hardware attached to the arm.

The second category alters the variable impedance by external devices such as grip force measurements or potentiometers excluding the knowledge of human anatomy for impedance estimation [8], [9], [17]. The first to aim a research on replicating human skills by using a user-controlled variable impedance

---

Stijn Klevering is with Delft Haptics Lab, Cognitive Robotics, Delft University of Technology, Mekelweg 2, 2628 CD Delft, The Netherlands (e-mail: stijn.klevering@gmail.com).

$^*$Corresponding author.

controller was Walker et al. 2010. This study showed that a natural strategy using grip force is simple and robust to utilize impedance variation and consequently control impact forces in varying contact tasks [8]. External devices are not subject to long calibration times. However, experimental applications enable a variable impedance in only one dimension and do not give the possibility for bimanual use due to an additional handheld device to control the impedance.

To implement a tele-impedance control architecture in teleoperation applications we have to take into account constraints for a successful design [3]. The implementation of tele-impedance may not hinder the ability for bimanual use, decrease dexterity, introduce long calibration times and may not obstruct the operator [5], [22]. EMG methods introduce long calibration times, obstruct the operator due to additional hardware attached to the arm and can introduce the coupling effect in combination with bilateral teleoperation [10], [23]. Existing methods using external devices do not have the ability to control a multi-dimensional variable impedance and no ability to use the secondary arm due to the additional handheld device [9]. Therefore, the existing tele-impedance interfaces are not optimal regarding adaptability to the environment or obstruction due to calibration and hardware.

To resolve the issue of both hands being occupied, the introduction of long calibration times, obstruction for the operator and the inability to control multi degrees of freedom variable impedance, we propose a novel tele-impedance control architecture for bimanual teleoperation applications in remote environments inspired by human arm stiffness ellipse modulation. The difference with existing methods is control of a two dimensional variable impedance operated by the foot with a new device called *the circular disc interface*.

Foot interfaces in literature have shown to give the ability to the operator to control a third manipulator or camera with their feet but no metrics for performance were used in these studies [24], [25]. On the other hand, Rudolph et al. 2019 evaluated the performance of an operator coordinating a robotic arm using their foot in a three-handed task. The experiment showed that human users could reliably use their foot to coordinate the motion of the robot [26]. In this paper, the circular disc interface does not directly control the position of the manipulator but controls a stiffness ellipse located at the end effector of a manipulator by rotation and elongation enabling tele-impedance control. The method introduces short calibration times, the ability for bimanual teleoperation and the ability for two dimensional impedance control. On the other hand, this method can introduce errors regarding rotation and elongation of the stiffness ellipse in comparison with the ideal stiffness ellipse configuration affected by the environment and task. Errors regarding the ideal stiffness ellipse configuration can be affected by the rotation of the ellipse as humans tend to overestimate angles during visual-haptic angle matching tasks while the human tends to underestimate angles during haptic-visual angle matching tasks [27].

Based on literature and the interface design we can hypothesize the following:

1) H1: The circular disc interface tele-impedance control method has a superior performance regarding force and position tracking in a dual task in comparison with constant impedance control for unilateral and bilateral control setting.
2) H2: The rotational accuracy of the disc interface negatively affects position and force tracking in a dual task.
3) H3: The circular disc interface tele-impedance control method has the ability to dynamically change the variable stiffness according to task instruction and situation.
4) H4: The circular disc interface introduces no increased overall effort of the operator.

We demonstrate the new control design with experiments in a virtual environment equipped with the Sigma.7 performing a drilling task while being exposed to force and position perturbations. To evaluate the effect of implementing the control architecture in bilateral and unilateral teleoperation, the experiment will be performed under two teleoperation settings; with and without force feedback. To evaluate the performance of the control design regarding interaction with the environment and position accuracy, three conditions will be evaluated; high uniform impedance, low uniform impedance and variable impedance controlled by the circular disc interface. Furthermore, the environment will be rotated providing the change of ideal stiffness ellipse strategy. Hereby, we evaluate the control accuracy of the circular disc interface by the operator relative to the optimal stiffness ellipse strategy. We also provide a subjective analysis to assess the overall workload during the drilling task.

## II. THEORETICAL BACKGROUND

This study developed and analyzed a novel tele-impedance control method for teleoperation including unilateral and bilateral teleoperation settings. During unilateral teleoperation, the control architecture will not feed any information back through the master device. During bilateral teleoperation the operator receives force feedback information through the master device. Since we were only interested in the performance regarding position and force tracking of the system during perturbations and not the corrupting effects of real-world bilateral teleoperation issues such as stability, time delay and transparency, we used a virtual impedance-controlled robotic manipulator and a virtual remote environment. Both were generated on the same computer that was used for control of the haptic device and variable impedance interface. Furthermore, we assumed that the robotic manipulator was perfectly gravity and inertia compensated. We are primarily focused on assessing the performance of the variable stiffness interface on the remote robot side since that is where the actual task exists. To have a reference to compare the variable stiffness method we included a constant high and low stiffness profile located at the end-effector. Additionally, we are interested in stiffness ellipse command and teleoperation in two degrees of freedom, therefore, we simplified 6 degrees of freedom teleoperation to 2 degrees of freedom.

### A. Tele-impedance control

Impedance control includes an approach that the controller implements a dynamic relation between end-point position

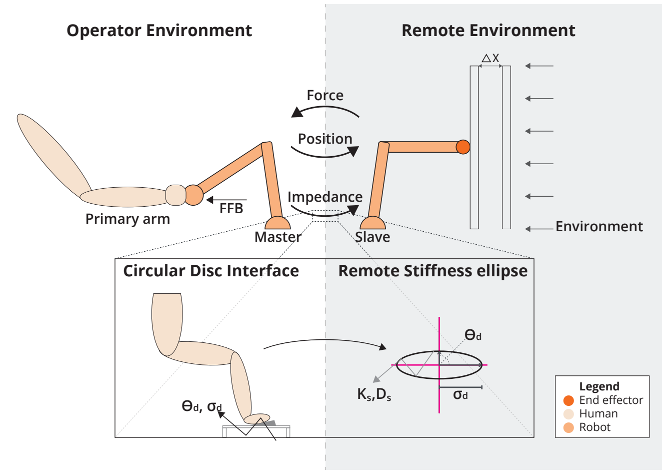

Fig. 1. Bilateral tele-impedance. The force feedback (FFB) is felt by the human operator. The FFB depends on the difference between reference position of the Master, actual position of the slave and stiffness profile. The operator controls the stiffness by the Circular Disc interface in two degrees of freedom. The system will not have force feedback with unilateral setting

and force rather than just control that variables [28]. A tele-impedance controlled teleoperation system can be unilateral, which only uses position and stiffness input, and bilateral, which includes force feedback to the master.

The study involved both bilateral and unilateral tele-impedance controlled methods illustrated in Fig. 1. The human operator controlled the reference position and a two dimensional stiffness ellipse of the remote virtual slave through a circular disc interface controlled by the foot. Depending on the bilateral or unilateral control, the operator receives force feedback from the interaction between slave and environment by the impedance control law [28]. The interaction force at the remote site depends on the impedance parameters and the difference between reference position (desired position) and actual position/motion of the slave as

$$\boldsymbol{f}_{ext} = \boldsymbol{K}(\boldsymbol{x}_d - \boldsymbol{x}_a) + \boldsymbol{D}(\dot{\boldsymbol{x}}_d - \dot{\boldsymbol{x}}_a), \tag{1}$$

where $\boldsymbol{f}_{ext} \in \mathbb{R}^3$ is the external force acting from the remote robot on the remote environment. Vector $\boldsymbol{x}_a \in \mathbb{R}^3$ is the actual position of the robotic manipulator end-effector and vector $\boldsymbol{x}_d \in \mathbb{R}^3$ is the desired end-effector position controlled by the master. $\boldsymbol{K} \in \mathbb{R}^{3\times3}$ and $\boldsymbol{D} \in \mathbb{R}^{3\times3}$ are the commanded stiffness and damping matrix. Since the interaction force between end-effector and environment is calculated by $\boldsymbol{f}_{ext}$ this variable will be fed back during bilateral teleoperation, not with unilateral teleoperation. The damping matrix stabilized the system and was defined as a function of the commanded stiffness matrix as

$$\boldsymbol{D} = 2\zeta\sqrt{\boldsymbol{K}}. \tag{2}$$

The damping coefficient $\zeta$ was set to 0.7 to make the system critically damped [29]. A critical damping helps to return the system into equilibrium without large overshoots and oscillations.

### B. Human limb stiffness ellipse modulation

Tele-impedance enables the operator to control a variable impedance located at the end-effector conducted by impedance control. There is evidence in literature that a comparable strategy to impedance control exists in motion control in biological systems [16], [30]. The variable end-point impedance of a human limb depends on the type of task humans have to perform and what kind of environmental perturbation is applied to the arm [15]. The human limb end-point stiffness profile will eventually be produced by excitatory or inhibitory muscle Golgi tendon force feedback, co-contraction and muscle spindle feedback [14]. Behavior of human arm impedance substantially depends on task instruction. Force tasks generally induce a decrease of human arm stiffness to accurately control a reference force [31]. During position tasks, the human operator increases the impedance to hold posture and effectively reject any perturbation. This is especially the case when low-frequent force perturbations were presented [14].

The human limb end-point stiffness profile can generally be described as a stiffness ellipse. The stiffness ellipse depends on posture and viscoelastic limb properties controlled by muscle contraction. Various studies provide stiffness measurements and estimations and describe a human limb end-point stiffness ellipse [16], [32], [33]. The endpoint stiffness matrix can be calculated from the joint stiffness matrix as

$$\boldsymbol{K} = \boldsymbol{J}^{-T}(\boldsymbol{q})\boldsymbol{K}_J\boldsymbol{J}^{-1}(\boldsymbol{q}), \tag{3}$$

with $\boldsymbol{K} \in \mathbb{R}^{6\times6}$ is the endpoint stiffness matrix of the human arm and $\boldsymbol{K}_J \in \mathbb{R}^{n\times n}$ is the stiffness matrix, with n the degrees of freedom of the join-space. $\boldsymbol{J}(\boldsymbol{q}) \in \mathbb{R}^{6\times n}$ is the limb Jacobian, which represents the postural dependency, where $\boldsymbol{q} \in \mathbb{R}^6$ is the joint configuration. To describe the stiffness matrix in a stiffness ellipse, singular vectors and non-zero singular values have to be obtained by the Singular Value Decomposition (SVD) described by

$$\boldsymbol{K} = \boldsymbol{U}\boldsymbol{E}\boldsymbol{V}^T, \tag{4}$$

where $\boldsymbol{K} \in \mathbb{R}^{6\times6}$ is the endpoint stiffness matrix of the human arm [16], [34]. $\boldsymbol{U} \in \mathbb{R}^{6\times6}$ and $\boldsymbol{V} \in \mathbb{R}^{6\times6}$ are the matrices representing rotations of the stiffness ellipse. $\boldsymbol{E} \in \mathbb{R}^{6\times6}$ is a diagonal matrix and represents the scaling of the semi-major and semi-minor axis of the stiffness ellipse by factor $\sigma_i$.

## III. INTERFACE DESIGN

We designed a novel foot-operated circular disc interface that has two inputs; a rotating part that enables rotating a stiffness ellipse and a foot pad that enables elongation of the stiffness ellipse illustrated in Fig. 2. This gives the operator the ability to adjust the stiffness ellipse in one 2D plane in real-time.

### A. Design requirements

To support the demands for a successful tele-impedance interface design, the following requirements have to be met:

1) R1) The operator's arm must not be obstructed by the stiffness command interface

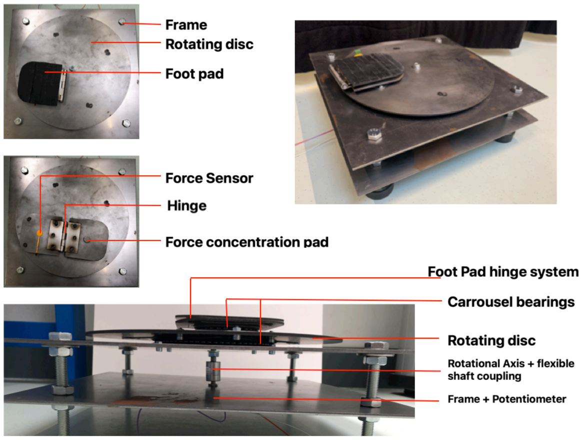

Fig. 2. An overview of the circular disc interface design. The top left corner shows the top view of the device with the hinged pad closed. The middle figure on the left shows the top view of the device with the hinged pad open to show the force sensor and force concentration pad. The bottom figure shows a side view of the device to show the positions of the carousel bearings, rotational axis and flexible shaft coupling with the potentiometer attached under the frame to the rotational axis.

2) R2) Enables stiffness commands in more than one DOF
3) R3) The design does not involve long calibration procedures and knowledge of human anatomy
4) R4) The design does not introduce the coupling effect between force-feedback and commanded stiffness.

Interfaces in walker et al. 2010, walker et al. 2012 and peternel et al. 2015 fail to meet R1 and R2, because of the need of an additional hand held device to regulate the impedance of the manipulator only in one dimension. The likelihood that an operator will use a tele-impedance device depends on the level that the system will support or hinder their work [35]. Therefore, the system design should minimize calibration times and additional hardware attached to the operator is undesirable. Interfaces in Adjoudani 2012, 2014 and Huang et al. 2017 failed to meet R3 and R4, because of the use of EMG interfaces, which involved long calibration procedures and knowledge of the human anatomy. Furthermore, the use of EMG interfaces introduce the coupling effect between force-feedback and commanded stiffness. Therefore, EMG interfaces will not be an option to meet the requirements.

### *B. Tele-impedance interface design*

To meet all the requirements stated before, an interface called “Circular disc interface” has been created, which was approved by the Human Research Ethics Committee of TU Delft. The device has the ability to control a stiffness ellipse located at the end-point of the manipulator with the foot. Using the Singular Value Decomposition from (4) we are able to generate a stiffness ellipse by two inputs as

$$\boldsymbol{K} = \boldsymbol{U}\boldsymbol{E}\boldsymbol{U}^T, \tag{5}$$

where $\boldsymbol{K} \in \mathbb{R}^{2\times2}$ is the stiffness matrix. $\boldsymbol{U} \in \mathbb{R}^{2\times2}$ is the matrix representing the rotation of the ellipse by Euler angles with

$$\boldsymbol{U} = \begin{bmatrix} cos(\theta) & -sin(\theta) \\ sin(\theta) & cos(\theta) \end{bmatrix}, \tag{6}$$

with $\theta \in \mathbb{R}^1$ the rotation angle of the ellipse. $\boldsymbol{E} \in \mathbb{R}^{2\times2}$ represents the scaling of the stiffness ellipse by

$$\boldsymbol{E} = \begin{bmatrix} \sigma_1 & 0 \\ 0 & \sigma_2 \end{bmatrix}, \tag{7}$$

with $\sigma_1 \in \mathbb{R}^1$ the scaling of the semi-major axis and $\sigma_2 \in \mathbb{R}^1$ the scaling of the semi-minor axis. To control the stiffness ellipse, the circular disc interface controls $\theta$ and $\sigma_1$ to create the ability to control the stiffness in all directions with minimum input. $\sigma - 2$ can be changed by switching the modes or can be indirectly controlled through a ratio between $\sigma_1$ and $\sigma_2$. During the experiments the latter was used by a $\sigma_2$ that remains constant at minimum stiffness.

The circular disc is connected to a rotating potentiometer for control of the rotation of the ellipse shown in Fig. 3. The rotation of the circular disc has a linear relationship with the rotation of the ellipse. Furthermore, a force sensor is attached under the foot pedal using a hinge system to exert the force at the force sensor, which controls the semi-major axis of the stiffness ellipse. The control of rotation and shape will be applied in the global frame, meaning that rotating the endpoint of the manipulator will not rotate the stiffness ellipse. This gives the ability for the operator to use multiple types of tools attached to the manipulator e.g. graspers or drills. Furthermore, rotation in the global frame will provide a reference between circular disc interface configuration and stiffness ellipse configuration when the stiffness ellipse is not visualized. Consequently, it can be used for multiple applications, tasks and environments.

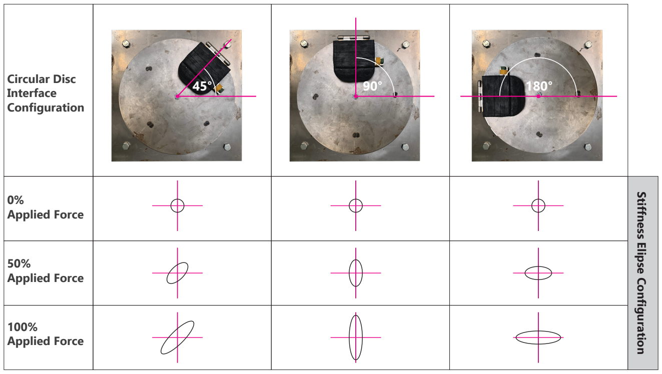
Circular Disc Interface Configuration
45°
90°
180°
0% Applied Force
50% Applied Force
100% Applied Force
Stiffness Ellipse Configuration

Fig. 3. The relation between the configuration of the Circular Disc interface configuration and stiffness ellipse configuration

The interface of the circular disc uses a rotational potentiometer mounted under the structure attached to a shaft, a shaft coupler to compensate for misalignment and the disc on top of the device. The circular disc rotates around the shaft stabilized by a carousel bearing and the main frame. To control rotation of the disc a foot pad is attached to the circular disc by a carousel bearing to enable rotation of the foot while rotating the disc resulting in a stable movement of the foot. The rotation of the circular disc has a linear relationship with the rotation of the ellipse. The input of the potentiometer is 0 Volts for -70 degrees and 5 Volts for 250 degrees shown in figure 3. The potentiometer only has the ability to measure between -

160 and 160 degrees of rotation. The rotation of the stiffness ellipse will be calculated as

$$\theta = \frac{V_\theta}{V_{\theta,max} - V_{\theta,min}}(\theta_{max} - \theta_{min}) + \theta_c, \tag{8}$$

with the rotation of the stiffness ellipse $\theta \in \mathbb{R}^1$ and $V_\theta \in \mathbb{R}^1$ the voltage output of the potentiometer. $V_{\theta,min} \in \mathbb{R}^1$ and $V_{\theta,max} \in \mathbb{R}^1$ the minimum and maximum voltage output. $\theta_{max} \in \mathbb{R}^1$ and $\theta_{min} \in \mathbb{R}^1$ the maximum and minimum rotation of the stiffness ellipse and $\theta_c \in \mathbb{R}^1$ a rotational correction to align the circular disc interface to the virtual stiffness ellipse.

Changing the shape of the ellipse will be done by elongating the semi-major axis controlled by a SingleTact force sensor under the foot pad shown in Fig. 3. The SingleTact force sensor can measure up to 450 Newton with a force resolution $<0.2\%$ of full scale and a repeatability error of $<1.0\%$ [36]. Force to voltage output has a linear relationship with $<0.2\%$ linearity error as

$$V_F = \frac{F_p}{F_{p,max}}(V_{F,max} - V_{F,min}), \tag{9}$$

where $V_F \in \mathbb{R}^1$ is the voltage output of the force sensor. $F_p \in \mathbb{R}^1$ is the force applied on the footpad by the operator and $F_{p,max} \in \mathbb{R}^1$ the maximum force defined by the force sensor. $V_{F,min} \in \mathbb{R}^1$ and $V_{F,max} \in \mathbb{R}^1$ are the maximum and minimum voltage output. The force sensor has a voltage output translated to semi-major axis scaling $\sigma_1 \in \mathbb{R}^1$ by

$$\sigma_1 = \frac{V_F - V_{F,min}}{V_{F,max} - V_{F,min}}(\sigma_{1,max} - \sigma_{1,min}) + \sigma_{1,min}, \tag{10}$$

where $\sigma_{1,max} \in \mathbb{R}^1$ and $\sigma_{1,min} \in \mathbb{R}^1$ are the maximum and minimum stiffness. We include if-statements regarding $\sigma_1$ so the semi-major axis cannot become larger or smaller than $\sigma_{1,max}$ and $\sigma_{1,min}$.

## IV. EXPERIMENT METHODS

### A. Participants

In total, 12 male participants between 21 and 36 years old (M = 24.8, SD = 4) participated in the experiment. One of the participants had minor experience with teleoperation. Their participation was voluntary and their efforts were not financially compensated for. All experiment protocols were approved by the Human Research Ethics Committee of TU Delft and all research was performed in accordance with relevant guidelines and regulations. All subjects gave a written informed consent prior to their participation.

### B. Experiment setup

To test the hypothesis for the circular disc interface control method we designed a dual teleoperation task in the form of a drilling in a wall task in a two dimensional plane. The drilling task was divided in two phases; phase 1 was a finding the hole task and phase 2 the drill insertion task. The participant performed the drilling task with two teleoperation settings including unilateral control and bilateral control. To assess the performance of the circular disc interface control method, we compared three impedance conditions applied to the end-effector of the virtual manipulator including high uniform impedance, low uniform impedance and variable impedance controlled by the circular disc interface. The high and low uniform stiffness of the stiffness ellipse located at the end-effector were determined in pilot studies to be 1500 N/m and 200 N/m. To evaluate the performance of the participant regarding accuracy of intended stiffness ellipse rotation in comparison with ideas stiffness ellipse orientation, we rotated the environment (-20, -10, 0, 10 ,20 degrees) to induce the participant to rotate the ellipse according to environment and task instruction.

The experiment setup is show in Fig. 4. We used a 7 DoF Force Dimension Sigma.7 haptic device to teleoperate a virtual remote manipulator. The sigma.7 was gravity and inertia compensated. We examined translational movements in the x and y direction and rotational movement around the z-axis. Translational movement in the z-axis and rotational movement around the x and y axis has not been constraint. Instead of constraints a visual indicator has been applied to warn the participant if he/she was out of the limits of the unexamined movements of the robot. The visual indicator consisted out of a change of color of the virtual manipulator from green to red. A monitor was used to display the commanded virtual drill, virtual environment and a reference force parallel to insertion direction of the drill in real-time shown in Fig. 5.

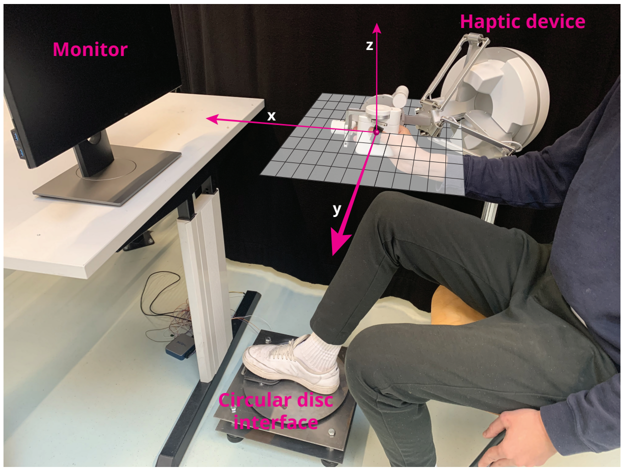

Fig. 4. Illustration of experiment setup. The participant controlled the Sigma.7 haptic device with the right arm. The participant commanded remote robot stiffness by the circular disc interface. The end-effector of the remote robot and the virtual environment including the force applied on the environment in insertion direction was displayed on the monitor in front of the participant.

The drilling task consists out of two phases shown in Fig. 5. In the first phase, called “Finding the hole phase”, the participant was instructed to continuously press on the wall with 10 Newton reference force for 10 seconds. On top of that, the participant was instructed to hold the position at the reference position indicated by a black surface area on the wall. During maintaining the reference force and position, the slave was subjected to a multi-sine force perturbation perpendicular to insertion direction. The wall indicated that the task was completed by changing color from green to red. Subsequently, the participant had to move the master back to a position located at the negative x-axis of the master to activate the second phase. For the second phase called "drill insertion phase", the participant had to drill a hole in the wall. Similar to the finding the hole phase, the position of drill insertion was indicated by a black surface area on the wall. The participant had to maintain the optimal drilling force of 10 N in insertion direction and was instructed to minimize forces on the wall in perpendicular direction of drill insertion while the drill was inserted. During the drill insertion, the wall was subjected to a multi-sine position perturbation perpendicular to insertion direction. The circular disc interface is used to control the stiffness ellipse located at the end-effector of the virtual manipulator.

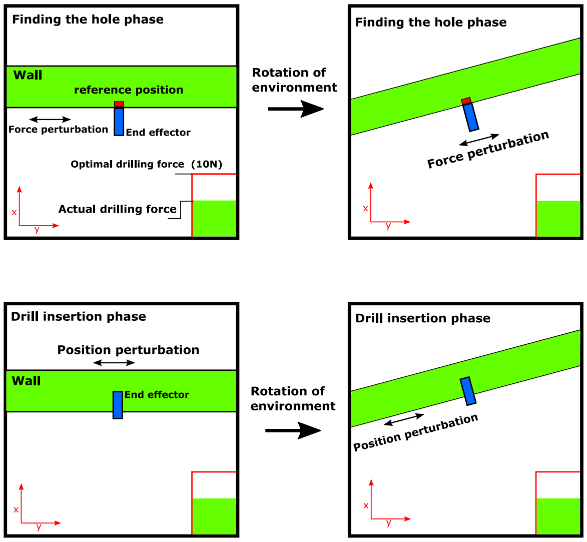

Fig. 5. The virtual environment with the virtual end-effector of the manipulator is shown. The top two figures show the finding the hole phase with force perturbation direction on the slave and a rotation of the environment. The bottom two figures show the drill insertion phase with positional perturbation direction on the environment and the difference in rotation of environment.

The input of the circular disc interface controlled variables for the singular value decomposition to change the stiffness ellipse from (5) and (7)-(10). $\sigma_2$ is the uniform low stiffness value for the semi-minor axis and the semi-major axis was variable and controlled by the force input of the circular disc interface by (10), which had a value between the uniform low impedance and the uniform high impedance values. The rotation of the ellipse is calculated by (8).During interaction with the environment, the stiffness of the manipulator and environment will interact in series resulting in a total stiffness as

$$\frac{1}{K_t} = \frac{1}{K_e} + \frac{1}{K_w}, \tag{11}$$

with $K_t$ the total stiffness, $K_e$ the stiffness of the stiffness ellipse and $K_w$ the stiffness of the environment. We assume that $K_w$ is infinitely stiff and therefore it becomes:

$$K_t = K_e, \tag{12}$$

which indicates that the infinitely stiffness environment does not have an influence on the total stiffness of the interaction between tool and environment.

The signals from the device were sampled at 1 kHz with a National Instruments DAQ device. During real-time processing, the signal was low-pass filtered (2nd order Butterworth, cut-off frequency of 5 Hz) introducing minor delay, which was not detrimental for controlling the stiffness ellipse and stability for the overall system. Input from the Sigma.7 and the circular disc interface were processed in Visual studio C++ and send to Matlab/Simulink by UDP with 100Hz. Matlab/Simulink visualized the environment, manipulator and interaction force in real-time on a display and stored the data.

### C. *Experiment protocol*

During the experiments, the participant was seated in a chair in front of the Sigma.7 device and the monitor. The Sigma.7 was adjusted to match the height for comfortable 90° of elbow flexion like in Fig. 4. Before the experiment, the participant was familiarized with teleoperation and the stiffness commanding methods. First, an understanding session was performed. The understanding session consisted out of getting familiarized with the environment with and without force feedback by performing the drilling task without perturbations under high and low stiffness condition. Next, a 1 degrees of freedom variable stiffness, controlled by the force pad of the circular disc interface, was introduced to let the participant feel the impact of a variable impedance. Thereafter, the stiffness ellipse control was introduced and explained. After thorough explanation of the variable stiffness ellipse, the participant performed the drilling task, including the variable stiffness ellipse control with the circular disc interface, with and without perturbations. When the observer of the experiment decided that the participant understood the impacts of tele-impedance and how to control telemanipulation and the circular disc interface, the participant performed the experiment with and without perturbations. First, with high and low uniform impedance, which will introduce the benefits and drawbacks of both methods. A variable stiffness ellipse strategy was created with the observer to create a well-founded understanding of variable stiffness strategies. Subsequently, a training session was performed to minimize the effects of learning. One training trial was performed for every impedance condition and force feedback setting during the training phase resulting in 6 training trials. The training was similar to the experiment trial, with random orientation of the environment.

The experiment sessions involved two force feedback settings (unilateral and bilateral setting) and 3 impedance conditions (High uniform impedance, Low uniform impedance and variable impedance). During each combination of setting and condition, 5 rotations of the environment (-20, -10, 0, 10, 20 degrees) were used. Therefore, the total amount of sessions consisting of 2 settings and 3 conditions and 5 rotations, resulted a total of 30 trials per participant. The understanding session lasted 20 to 25 minutes and the training session 15 to 25 minutes depending on the learning curve of the participant. The actual experiment took 60 minutes. The total duration of the experiment took 95 to 110 minutes. To diminish learning effects, we randomized the order of settings, conditions and the rotations of the environment based on Latin Square.

### D. Dependent measures

To determine the dependent measures we split up the data within sessions of the drilling task in data for the finding hole task and insertion task. Data used for the finding the hole task was defined by the time vector from reaching 10N reference force to the end of the task. The data used for the insertion task was defined by the time vector from start of position perturbation of the wall to reaching the end of the wall. For both data sets we aligned all data at the beginning of the time vectors.

During finding the hole task we looked at the primary (position perpendicular to insertion direction) and secondary (force in insertion direction) task performance. During the insertion task we looked at the primary (force perpendicular to insertion direction) and secondary (force in insertion direction) task performance. In each case we looked at the stiffness ellipse configuration and subjective results from the NASA TLX form.

*Finding the hole phase:* We quantified task performance as the average of the mean of the absolute error between the signal and a reference position or force. We quantified the ellipse performance as the average of the mean of the rotational error between rotation of ellipse and ideal rotation of ellipse (stated in part …). In the following definitions, err and ref are respectively error and reference. N is the length of the corresponding time-vector. For the finding the hole phase we used the following metrics:

$$\textit{Mean absolute position error} : \bar{\boldsymbol{x}}_{err} = \frac{\sum |\boldsymbol{x}_a - \boldsymbol{x}_{ref}|}{N}$$

$$\textit{Root mean square force error} : \bar{\boldsymbol{F}}_{err} = \frac{\sqrt{\sum (\boldsymbol{F}_a - \boldsymbol{F}_{ref})^2}}{N}$$

The reference of rotation of the ellipse depends on the rotation of the wall in the global frame. To take into account the symmetry of the ellipse, we correct the ellipse by 180 degrees to have all rotations in the same part of the frame. Since rotating the ellipse by 180 degrees created exactly the same ellipse, we can rotate the ellipse by 180 degrees to compare rotations with each other for different strategies. $\theta_{ref}$ is the rotation of the ellipse in the following definition.

$$\textit{Mean rotation} : \bar{\theta}_a = \frac{\sum \theta_a}{N}$$

$$\textit{Correction} : if \;\; \bar{\theta}_a < -90^\circ$$

$$\bar{\theta}_a = \bar{\theta}_a + 180^\circ$$

$$\textit{Mean rotation error} : \bar{\theta}_{err} = \bar{\theta}_a - \theta_{ref}$$

*Insertion phase:* During the insertion phase there could be a high probability for damage of the tool or environment with high force peaks. Therefore, we used the Root mean square error of the force perpendicular to insertion direction to include a larger weighting of force peaks, which increase the possibility of damaging the environment or tool. During the insertion phase the following metrics were used:

$$\textit{RMSE of force} : \bar{\boldsymbol{F}}_{err} = \sqrt{\frac{\sum (\boldsymbol{F}_a - \boldsymbol{F}_{ref})^2}{N}}$$

$$\textit{RMSE of force} : \bar{\boldsymbol{F}}_{err} = \sqrt{\frac{\sum (\boldsymbol{F}_a - \boldsymbol{F}_{ref})^2}{N}}$$

*Subjective analysis:* A NASA TLX form had to be filled in by the participant between sessions. In total 6 TLX forms for every control setting and condition per participant.

### E. Statistical Analysis

An ANOVA test was performed for the statistical analysis. A significance level of $p \leq 0.05$ is considered as a significant difference. Because we are performing multiple analysis on the dataset corresponding to force and position tasks we use a Bonferroni correction, which compensated for the increased chance of committing a Type 1 error. Afterwards we conducted a t-test on significant results to compensate for the increased chance of committing a Type 2 error due to the multiple comparisons with Bonferroni correction.

## V. RESULTS

The understanding and training phase of the drilling task were not analyzed. The next paragraphs show the results of the effect of the circular disc interface on the drilling task regarding interaction performance with the environment during phase 1 (finding the hole task), phase 2 (drill insertion task) and commanded stiffness accuracy. Furthermore, a subjective analysis is presented.

TABLE I
OVERVIEW OF ANOVA RESULTS OF THE FINDING THE HOLE PHASE FOR BOTH POSITION ERROR AND FORCE ERROR.[1]

| | Position error | | | Force error | | |
|---|---|---|---|---|---|---|
| Source | d.f. | F | p | d.f. | F | p |
| IMP | 2 | 799.12 | <.001 | 2 | 37.93 | <.001 |
| FFB | 1 | 746.93 | <.001 | 1 | 5.18 | .024 |
| ROT | 4 | 2.73 | .029 | 4 | 3.24 | .013 |
| IMP*FFB | 2 | 3.73 | .025 | 2 | 1.55 | .214 |
| IMP*ROT | 8 | 0.68 | .071 | 8 | 1.73 | .091 |
| FFB*ROT | 4 | 1.16 | .330 | 4 | 2.18 | .071 |
| Error | 338 | | | 338 | | |

[1] In the table, IMP is impedance mode (High uniform, low uniform and variable impedance), FFB is force feedback setting (bilateral and unilateral) and ROT are the rotations of the environment (-20, -10, 0, 10, 20 degrees). The position error is perpendicular to insertion direction and the force error parallel to insertion direction.

### A. Finding the hole phase

An N-way ANOVA was conducted to compare the mean absolute position error and root mean square force error between teleoperation control methods, impedance modes and rotations of the environment. Subsequently a multicomparison test was done with Bonferroni correction. Table I shows the ANOVA results of both dependent measures. The top figure of Fig. 6 shows the absolute position error for the finding the hole phase with force feedback setting and impedance mode. The bottom graph of Fig. 6 shows the root mean square error of the interaction force.

The ANOVA with Impedance mode (high uniform, low uniform and variable impedance) and force feedback settings (bilateral and unilateral) on position error perpendicular to

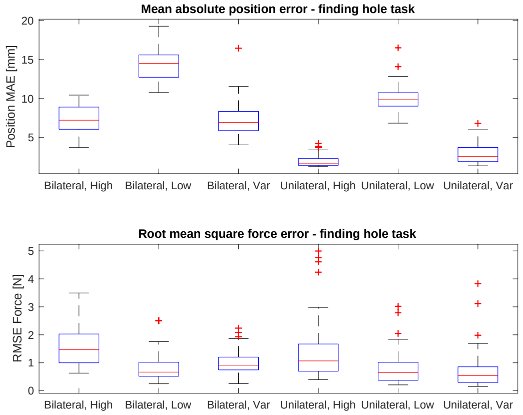

Fig. 6. The mean absolute position error during finding the hole task in the top figure and the root mean square of the force error during finding the hole task for force feedback setting and impedance control conditions.

insertion direction revealed a main effect of impedance mode, F(2,338) = 799, p<.001 and a main effect of force feedback setting, F(1,338), p<.001. This was qualified by the interaction between Impedance mode and force feedback setting, F(2,338) = 3.73, p = .025. Post-hoc analyses using multicomparisons with Bonferroni correction indicated that the position errors were lower for variable impedance mode than for low uniform impedance mode during bilateral setting (p<.001). The same holds for unilateral setting (p<.001). No significant difference was found between high uniform impedance and variable impedance mode during bilateral setting but for unilateral setting a significant higher position error for variable impedance mode in comparison with high impedance mode was found (p = .002). Furthermore, the effect of force feedback during variable impedance mode yielded a lower position error for unilateral setting than for bilateral setting, p<.001.

The ANOVA with impedance mode (high uniform, low uniform and variable impedance) and force feedback settings (bilateral and unilateral) on force error parallel to insertion direction revealed a main effect of impedance mode, F(2,338) = 37.93, p<.001 and a main effect of force feedback setting, F(1,338) p = .024. No significant interaction was found between impedance mode and force feedback setting F(2,338), p = 0.21. Post-hoc analyses using Bonferroni correction indicated that the force errors were lower for variable impedance mode than for high impedance mode (p<.001). Furthermore, larger force errors were found for bilateral teleoperation than for unilateral teleoperation (p=.0235).

### *B. Drill insertion phase*

An N-way ANOVA was conducted to compare the root mean square force error perpendicular to insertion direction and root mean square force error parallel to insertion direction between teleoperation control methods, impedance modes and rotations of the environment. Subsequently a multicomparisons test was done with Bonferroni correction. Table II shows the ANOVA results of both dependent measures. The top figure of Fig. 7 shows the mean squared force error perpendicular in insertion direction for the drill insertion phase for teleoperation setting and impedance control. The bottom graph of Fig. 7 shows the root mean square error parallel to insertion direction for the drill insertion phase.

TABLE II
OVERVIEW OF ANOVA RESULTS OF THE DRILL INSERTION PHASE FOR BOTH PARALLEL AND PERPENDICULAR FORCE ERROR.[2]

| | Perpendicular Force error | | | Parallel Force error | | |
|---|---|---|---|---|---|---|
| Source | d.f. | F | p>F | d.f. | F | p>F |
| IMP | 2 | 407.61 | <.001 | 2 | 11.49 | <.001 |
| FFB | 1 | .88 | .349 | 1 | .020 | .875 |
| ROT | 4 | 1.28 | .277 | 4 | .86 | .490 |
| IMP*FFB | 2 | 2.02 | .134 | 2 | 4.60 | .011 |
| IMP*ROT | 8 | 1.82 | .072 | 8 | 1.34 | .222 |
| FFB*ROT | 4 | .470 | .756 | 4 | 1.07 | .371 |
| Error | 338 | | | 338 | | |

[1] In the table, IMP is impedance mode (High uniform, low uniform and variable impedance), FFB is force feedback setting (bilateral and unilateral) and ROT are the rotations of the environment (-20, -10, 0, 10, 20 degrees). The parallel force error is the error considering the optimal drilling reference force of 10N.

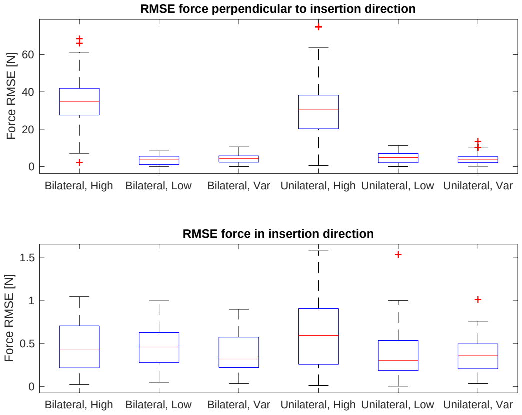

Fig. 7. The mean root mean square error error during the drill insertion task in the top figure and the root mean square of the force error during finding the hole task for force feedback setting and impedance control conditions.

The ANOVA with Impedance mode (high uniform, low uniform and variable impedance) and force feedback settings (bilateral and unilateral) on force error perpendicular to insertion direction revealed a main effect of impedance mode, F(2,338) = 408, p<.001 but no main effect of force feedback setting, F(1,338)=.88, p = .35. No significant interaction was found between impedance mode and force feedback setting F(2,338)=2.02, p=0.134. Post-hoc analyses using multicomparisons with Bonferroni correction indicated that the force errors were lower for variable impedance mode than for high uniform impedance mode during both force feedback settings (p<.001). No significant difference was found between low uniform impedance and variable impedance mode.

The ANOVA with Impedance mode (high uniform, low uniform and variable impedance) and force feedback settings (bilateral and unilateral) on force error parallel to insertion direction revealed a main effect of impedance mode, F(2,338) = 11.5, p<.001 but no main effect of force feedback setting, F(1,338)=.02, p = .88. This was qualified by the interaction between impedance mode and force feedback setting F(2,338)=4.60, p = 0.011. Post-hoc analyses using multicomparisons with Bonferroni correction indicated that the force errors were lower for variable impedance mode than for high uniform impedance mode during unilateral setting (p<.001). No significant difference was found between low uniform impedance and variable impedance mode during bilateral setting. No significant differences were found between low uniform impedance mode and variable impedance mode for both force feedback settings.

### C. Rotational errors

During variable impedance mode, the operator can make rotational errors in comparison with the ideal stiffness ellipse rotation, which can influence the performance regarding position and force errors. Therefore, we evaluated by an ANOVA the influence of rotation of the environment (-20, -10, 0, 10, 20 degrees) and force feedback settings (bilateral and unilateral) on rotation errors. The ANOVA did not find any significant effects of environment rotation and force feedback setting on the rotational error of the stiffness ellipse in comparison with ideal stiffness ellipse strategy.

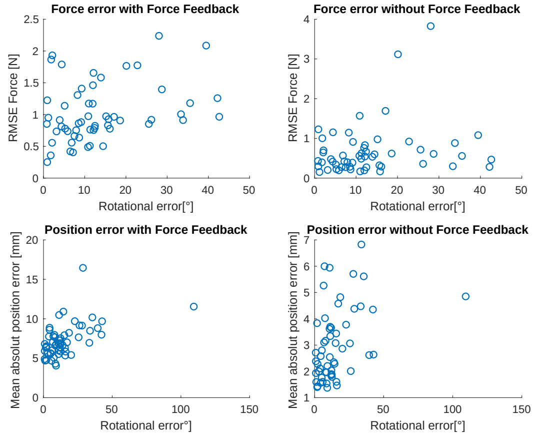

Fig. 8. The root mean square error and position error during the finding the hole phase are plotted against the rotational error of the stiffness ellipse in comparison with the ideal stiffness ellipse rotation. The first column depicts bilateral setting and the second column unilateral setting. The first row shows the root mean square error and the second row the position error.

Additionally, we evaluated the influence of rotation error on the root mean square error in the force tracking task and the absolute mean of the position error with the Spearman correlation coefficient illustrated in Fig. 8. A significant correlation was obtained during bilateral teleoperation for the absolute mean error of the position with R = 0.53, p <0.001 and for unilateral teleoperation with R = 0.41, p = 0.0017. No significant correlation was found between the root mean square error of the force perpendicular to insertion direction and the rotational error of the stiffness ellipse.

### D. Subjective analysis

Fig. 9 shows the overall workload of the raw TLX between teleoperation settings and impedance conditions. The ANOVA results of the NASA TLX questionnaire shows a main effect between force feedback settings on overall workload F(1,66)=16.42, p<.001. No interaction between impedance mode and force feedback setting was found. Post-hoc analyses using multicomparisons with Bonferroni correction indicated that the overall workload was higher for bilateral setting than for unilateral setting (p<.001). Furthermore, no significant main effect of impedance modes on overall workload was found F(2,66)=.64, p=.529.

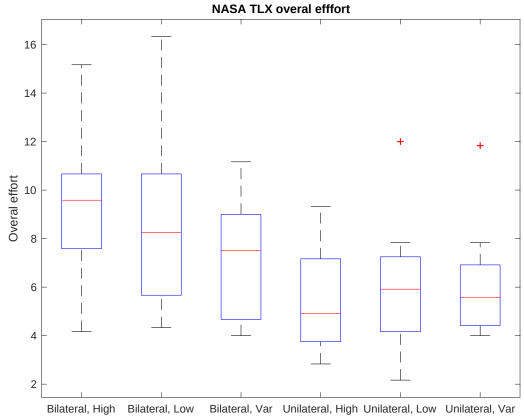

Fig. 9. The overall workload estimated by the RAW NASA TLX for impedance mode and force feedback setting.

## VI. DISCUSSION

### A. Design Results

This study introduced a novel tele-impedance interface design for teleoperation applications. The tele-impedance, called the circular disc interface, was controlled by the foot. This can be useful for bimanual teleoperation due to a free secondary hand meeting the requirements R1 and R4 in contrast to other proposed tele-impedance hand-held devices [8], [17], [31]. The circular disc interface controlled a stiffness ellipse based on human limb stiffness ellipse modulation. Other methods, using external devices to dynamically alter a variable impedance [8], [17], [31], enable the operator to change the robot impedance in a single axis of the Cartesian space or multiple axis at the same time. The method and interface proposed in this paper enables a variable impedance based on human limb stiffness ellipse modulation, which gives the operator the ability to alter the impedance in two dimensions of Cartesian space independently, fulfilling *R2*.

Tele-impedance methods using EMG and positional measurements do enable a multi-dimension variable impedance [10]–[12], [37]. However, these methods generally required long calibration times, additional knowledge of human anatomy and additional hardware including EMG sensors and markers. This adds up to a decrease of the probability for utilization and comfort of the operator. In contrast, the circular disc interface only required a calibration for rotational precision. Therefore, we were able to minimize calibration times and meet R3. Furthermore, no additional hardware attached to the operator was required meeting *R1*. On the other hand, participants needed a thorough explanation and training phase to understand the impact and strategies of the variable stiffness ellipse. This factor is contradictory to *R3*, due to the need of thorough understanding of variable stiffness ellipse strategies by the operator.

The tele-impedance control method was evaluated during unimanual teleoperation but has the capacity to be used for bimanual teleoperation due to a free secondary arm and foot. Therefore, we strongly recommend to further explore the influence of the interface design for bimanual teleoperation regarding position and force tracking performance and workload of the operator. The interface can also be used for altering a stiffness ellipse in three dimensions, where the interface can change the rotation and shape of the ellipse in multiple 2D planes independently by switching control modes by e.g. voice command [38]. Furthermore, the circular disc interface can be used for teaching methods [31], [37], [39] or human-robot co-manipulation [40] involving variable stiffness transfer in multiple degrees of freedom.

### B. *Experiment results*

Participants were able to command the rotation of the stiffness ellipse relative to the rotation of the environment and ideal stiffness ellipse strategy. The participant could accurately control the circular disc interface according to the task execution and environment. Therefore, the participant was able to dynamically adapt to a changing environment, performing position and force tracking tasks in multiple directions, which confirms hypothesis *H3*. This is consistent with results of dynamic adaptation in other tele-impedance studies [9], [10]

Ajoudani et al. 2018 performed a similar real-time drilling task with dynamic uncertainties succesfully with reduced complexity EMG measurements and position markers [18]. The study did not evaluate dependent measures such as interaction force or position. In contrast, the experiment conducted for the circular disc interface did evaluate dependent measures independent measures such as force feedback setting and impedance mode.

During the finding the hole phase for both unilateral and bilateral teleoperation, the circular disc interface allowed for significantly increased position tracking compared to low constant impedance control and significantly increased force tracking compared to the high constant impedance control. This suggests that tele-impedance control increases the interaction performance between tool and environment and increases tracking of a reference position in perpendicular direction for both teleoperation settings in comparison with constant uniform impedance control. This result confirms our hypothesis *H1*.

During the insertion phase, the participant let go of the circular disc interface to generate a low uniform stiffness required for the force tasks in parallel and perpendicular insertion direction. The end-effector was constraint by the environment and showed a low uniform impedance similarly as in [9]. During this phase, both the constant low impedance and variable impedance performed significantly better regarding force tracking in comparison with high uniform impedance during unilateral teleoperation. There was no significant difference of the force tracking error in insertion direction during bilateral teleoperation. This could be due to the introduction of human arm stiffness dynamics by force feedback. The performance analysis confirmed our hypothesis *H1*. This is especially true for the finding the hole phase but not for the drill insertion phase due to a similar performance between low uniform impedance and variable impedance. Since drilling tasks consist out of the two phases, we can confirm that our hypothesis *H1* is true for the drilling task.

Humans tend to underestimate angles on purely tactile judgement [27], [41]. This resulted in an error regarding the rotation based of the stiffness ellipse in comparison with the ideal rotation. On the other hand, there was no significant difference of the absolute rotation error between rotations of the environment. Furthermore, there was no relation between stiffness ellipse rotation error and force error in insertion direction during the finding the hole task. Small rotation errors between 10 or 20 degrees do not drastically increase the impedance in insertion direction. On top of that, the low rotation errors in combination with a low variability of force error do not have the ability to show a correlation between rotational error and force error. However, a moderate but significant correlation is shown between the rotational error and position error of R = 0.53 for bimanual teleoperation and R= 0.41 for unilateral teleoperation. This indicates that a accurate orientation of the stiffness ellipse is required to utilize the benefits of the circular disc interface for a position task. This result confirms hypothesis *H2* only for position tasks.

### C. *Subjective analysis*

The subjective analysis by the NASA TLX did not show a significant statistical difference of overall effort between impedance control conditions, which confirms hypothesis *H4*. This can be explained by an increase of effort due to the use of the circular disc interface but a decrease of effort by an easier task execution due to the introduction of the variable stiffness. Furthermore, participants experienced a statistically significant higher workload during bilateral teleoperation in comparison with unilateral teleoperation. This can be attributed to the force feedback introducing the need for applying force onto the master.

## VII. CONCLUSION

The novel design of the circular disc interface enables a two-dimensional variable tele-impedance control during unilateral an bilateral teleoperation. The interface was able to adapt the impedance according to task instruction and unpredictable environments in two dimensions. Consequently, the control interface improves interaction performance between tool and environment regarding force and position tracking in comparison with constant impedance controlled manipulators. The participants introduced rotational errors regarding the optimal stiffness ellipse configuration, which had minor detrimental effect on interaction performance. Furthermore, the control interface shows to have a larger impact on unilateral compared to bilateral teleoperation. Therefore, we recommend to use this control method especially in the case of unpredictable and unstructured unilateral tele-impedance task execution.

## REFERENCES

[1] B. Siciliano and O. Khatib, *Springer handbook of robotics*. Springer, 2016.

[2] L. Chan, F. Naghdy, and D. Stirling, "Application of adaptive controllers in teleoperation systems: A survey," *IEEE Transactions on Human-Machine Systems*, vol. 44, no. 3, pp. 337–352, 2014.

[3] S. Sivčev, J. Coleman, E. Omerdić, G. Dooly, and D. Toal, "Underwater manipulators: A review," *Ocean Engineering*, vol. 163, pp. 431–450, 2018.

[4] T. FOSSEN, K. Pettersen, and H. Nijmeijer, *SENSING AND CONTROL FOR AUTONOMOUS VEHICLES*. Springer, 2017.

[5] J. Yuh and M. West, "Underwater robotics," *Advanced Robotics*, vol. 15, no. 5, pp. 609–639, 2001.

[6] M. S. Johannes, R. S. Armiger, M. J. Zeher, M. V. Kozlowski, J. D. Bigelow, and S. D. Harshbarger, "Human capabilities projection: Dexterous robotic telemanipulation with haptic feedback," *Johns Hopkins APL Tech. Dig*, vol. 31, no. 4, pp. 315–324, 2013.

[7] R. D. Christ and R. L. Wernli Sr, *The ROV manual: a user guide for remotely operated vehicles*. Butterworth-Heinemann, 2013.

[8] D. S. Walker, R. P. Wilson, and G. Niemeyer, "User-controlled variable impedance teleoperation," in *2010 IEEE International Conference on Robotics and Automation*. IEEE, 2010, pp. 5352–5357.

[9] L. Peternel, T. Petrič, and J. Babič, "Human-in-the-loop approach for teaching robot assembly tasks using impedance control interface," *Proceedings - IEEE International Conference on Robotics and Automation*, vol. 2015-June, no. June, pp. 1497–1502, 2015.

[10] A. Ajoudani, N. G. Tsagarakis, and A. Bicchi, "Tele-impedance: Towards transferring human impedance regulation skills to robots," *Proceedings - IEEE International Conference on Robotics and Automation*, pp. 382–388, 2012.

[11] B. Huang, Z. Li, X. Wu, A. Ajoudani, A. Bicchi, and J. Liu, "Coordination Control of a Dual-Arm Exoskeleton Robot Using Human Impedance Transfer Skills," *IEEE Transactions on Systems, Man, and Cybernetics: Systems*, vol. 49, no. 5, pp. 954–963, 2017.

[12] L. Peternel, N. Tsagarakis, and A. Ajoudani, "A human-robot comanipulation approach based on human sensorimotor information," *IEEE Transactions on Neural Systems and Rehabilitation Engineering*, vol. 25, no. 7, pp. 811–822, 2017.

[13] A. Ajoudani, S. B. Godfrey, M. Bianchi, M. G. Catalano, G. Grioli, N. Tsagarakis, and A. Bicchi, "Exploring teleimpedance and tactile feedback for intuitive control of the pisa/IIT soft hand," *IEEE Transactions on Haptics*, vol. 7, no. 2, pp. 203–215, 2014.

[14] W. Mugge, D. A. Abbink, A. C. Schouten, J. P. Dewald, and F. C. Van Der Helm, "A rigorous model of reflex function indicates that position and force feedback are flexibly tuned to position and force tasks," *Experimental brain research*, vol. 200, no. 3, pp. 325–340, 2010.

[15] D. A. Abbink, "Task instruction: The largest influence on human operator motion control dynamics," in *Second Joint EuroHaptics Conference and Symposium on Haptic Interfaces for Virtual Environment and Teleoperator Systems (WHC'07)*. IEEE, 2007, pp. 206–211.

[16] J. Buzzi, G. Ferrigno, J. M. Jansma, and E. De Momi, "On the value of estimating human arm stiffness during virtual teleoperation with robotic manipulators," *Frontiers in neuroscience*, vol. 11, p. 528, 2017.

[17] D. S. Walker, J. K. Salisbury, and G. Niemeyer, "Demonstrating the benefits of variable impedance to telerobotic task execution," in *2011 IEEE International Conference on Robotics and Automation*. IEEE, 2011, pp. 1348–1353.

[18] A. Ajoudani, C. Fang, N. Tsagarakis, and A. Bicchi, "Reduced-complexity representation of the human arm active endpoint stiffness for supervisory control of remote manipulation," *The International Journal of Robotics Research*, vol. 37, no. 1, pp. 155–167, 2018.

[19] C. Fang, G. Rigano, N. Kashiri, A. Ajoudani, J. Lee, and N. Tsagarakis, "Online joint stiffness transfer from human arm to anthropomorphic arm," in *2018 IEEE International Conference on Systems, Man, and Cybernetics (SMC)*. IEEE, 2018, pp. 1457–1464.

[20] S. Park and W. K. Chung, "Tele-impedance control of virtual system with visual feedback to verify adaptation of unstable dynamics during reach-to-point tasks," in *2016 6th IEEE International Conference on Biomedical Robotics and Biomechatronics (BioRob)*. IEEE, 2016, pp. 1283–1289.

[21] J. Buzzi, A. Passoni, G. Mantoan, M. Mollura, and E. De Momi, "Biomimetic adaptive impedance control in physical human robot interaction," in *2018 7th IEEE International Conference on Biomedical Robotics and Biomechatronics (Biorob)*. IEEE, 2018, pp. 883–890.

[22] D. A. Abbink, T. Carlson, M. Mulder, J. C. De Winter, F. Aminravan, T. L. Gibo, and E. R. Boer, "A topology of shared control systems-finding common ground in diversity," *IEEE Transactions on Human-Machine Systems*, vol. 48, no. 5, pp. 509–525, 2018.

[23] L. M. Doornebosch, D. A. Abbink, and L. Peternel, "Analysis of coupling effect in human-commanded stiffness during bilateral tele-impedance," *IEEE Transactions on Robotics*, 2021.

[24] E. Abdi, E. Burdet, M. Bouri, and H. Bleuler, "Control of a supernumerary robotic hand by foot: An experimental study in virtual reality," *PloS one*, vol. 10, no. 7, p. e0134501, 2015.

[25] E. Abdi, M. Bouri, J. Olivier, and H. Bleuler, "Foot-controlled endoscope positioner for laparoscopy: Development of the master and slave interfaces," in *2016 4th International Conference on Robotics and Mechatronics (ICROM)*. IEEE, 2016, pp. 111–115.

[26] B. W. Rudolph, "Foot-controlled supernumerary robotic arm: Foot interfaces and human abilities," 2019.

[27] S. Appelle, "Visual and haptic angle perception in the matching task," *The American journal of psychology*, pp. 487–499, 1971.

[28] N. Hogan, "Impedance control: An approach to manipulation: Part ii—implementation," 1985.

[29] A. Albu-Schaffer, C. Ott, U. Frese, and G. Hirzinger, "Cartesian impedance control of redundant robots: Recent results with the dlr-light-weight-arms," in *2003 IEEE International conference on robotics and automation (Cat. No. 03CH37422)*, vol. 3. IEEE, 2003, pp. 3704–3709.

[30] P. K. Artemiadis, P. T. Katsiaris, M. V. Liarokapis, and K. J. Kyriakopoulos, "Human arm impedance: Characterization and modeling in 3d space," in *2010 IEEE/RSJ International Conference on Intelligent Robots and Systems*. IEEE, 2010, pp. 3103–3108.

[31] L. Peternel, T. Petrič, and J. Babič, "Robotic assembly solution by human-in-the-loop teaching method based on real-time stiffness modulation," *Autonomous Robots*, vol. 42, no. 1, pp. 1–17, 2018.

[32] T. Flash and F. Mussa-Ivaldi, "Human arm stiffness characteristics during the maintenance of posture," *Experimental brain research*, vol. 82, no. 2, pp. 315–326, 1990.

[33] H. Gomi and M. Kawato, "Human arm stiffness and equilibrium-point trajectory during multi-joint movement," *Biological cybernetics*, vol. 76, no. 3, pp. 163–171, 1997.

[34] J. McIntyre, F. Mussa-Ivaldi, and E. Bizzi, "The control of stable postures in the multijoint arm," *Experimental brain research*, vol. 110, no. 2, pp. 248–264, 1996.

[35] D. A. Abbink, T. Carlson, M. Mulder, J. C. de Winter, F. Aminravan, T. L. Gibo, and E. R. Boer, "A topology of shared control systems—finding common ground in diversity," *IEEE Transactions on Human-Machine Systems*, vol. 48, no. 5, pp. 509–525, 2018.

[36] Singletact 450n force sensor. [Online]. Available: https://www.singletact.com/micro-force-sensor/standard-sensors/15mm-standard-sensor/15mm-450newton/

[37] C. Yang, P. Liang, Z. Li, A. Ajoudani, C.-Y. Su, and A. Bicchi, "Teaching by demonstration on dual-arm robot using variable stiffness transferring," in *2015 IEEE International Conference on Robotics and Biomimetics (ROBIO)*. IEEE, 2015, pp. 1202–1208.

[38] M. Ferre, J. Macias-Guarasa, R. Aracil, and A. Barrientos, "Voice command generation for teleoperated robot systems," in *7th IEEE International Workshop on Robot and Human Communication 1998 (RO-MAN'98)*, vol. 2, 1998, pp. 679–685.

[39] C. Yang, P. Liang, A. Ajoudani, Z. Li, and A. Bicchi, "Development of a robotic teaching interface for human to human skill transfer," in *2016 IEEE/RSJ International Conference on Intelligent Robots and Systems (IROS)*. IEEE, 2016, pp. 710–716.

[40] L. Peternel, T. Petrič, E. Oztop, and J. Babič, "Teaching robots to cooperate with humans in dynamic manipulation tasks based on multi-modal human-in-the-loop approach," *Autonomous robots*, vol. 36, no. 1, pp. 123–136, 2014.

[41] S. Lakatos and L. E. Marks, "Haptic underestimation of angular extent," *Perception*, vol. 27, no. 6, pp. 737–754, 1998.

# A

# Tele-impedance control architecture

## A.1. Assumptions

Impedance control of a robotic system introduces a dynamic relation between end-point position and force. Due to the circular disc interface, the operator has the ability to dynamically alter the relation between position and force by changing the impedance illustrated in Fig. A.1. Since we are only interested in the performance regarding position and force tracking and not the corrupting effects of real world teleoperation systems, we used a virtual impedance-controlled manipulator and a virtual environment. To create the control architecture for the slave and environment we assumed that the slave was perfectly inertia and gravity compensated. Furthermore, we assumed no friction would occur between manipulator and environment.

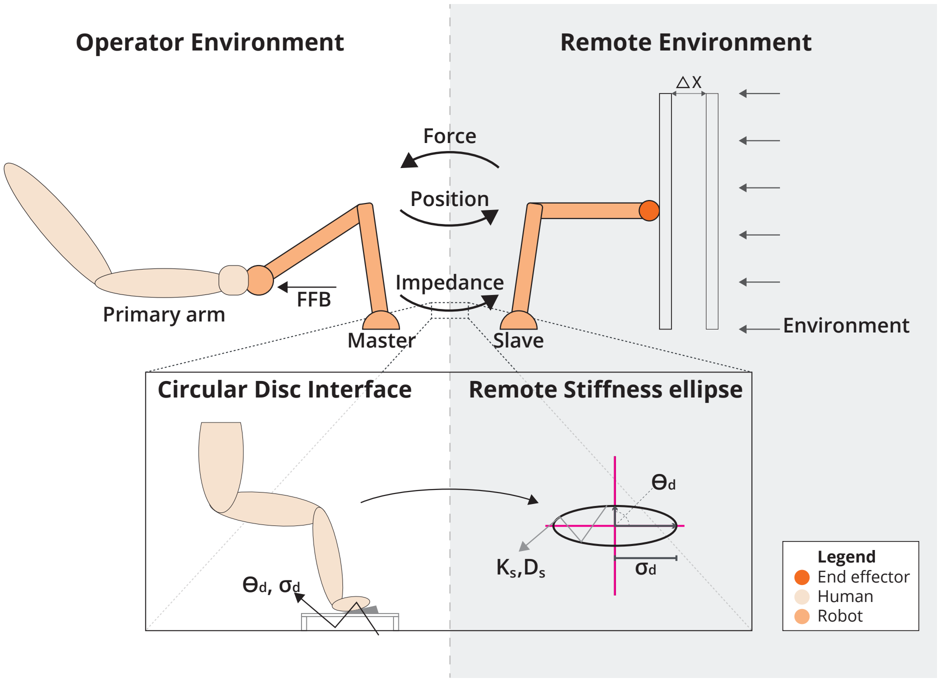
Operator Environment
Remote Environment
△X
Force
Position
Impedance
FFB
Primary arm
Master
Slave
Environment
Circular Disc Interface
Remote Stiffness ellipse
ϴd
ϴd, σd
Ks,Ds
σd
Legend
End effector
Human
Robot

Figure A.1: Bilateral tele-impedance. The force feedback (FFB) is felt by the human operator and is calculated by (A.2) or (A.3) depending on situation. The FFB depends on the difference between reference position of the Master, actual position of the slave and stiffness profile. The operator controls the stiffness by the Circular Disc interface in two degrees of freedom.

## A.2. Bilateral and Unilateral teleoperation

The experiment is conducted during bilateral and unilateral teleoperation settings. The interaction force between tool and environment located at the end-effector of the slave will be fed back to the master console during bilateral teleoperation. Because both virtual manipulator and virtual environment were generated on the same computer, negligible time delays were present, which can be detrimental for transparency and stability of the system, which takes the experimental focus away from real world teleoperation corrupting effects [8, 13, 17, 22]. Fig. A.2 depicts the bilateral and teleoperation control architecture for the experiment setup.

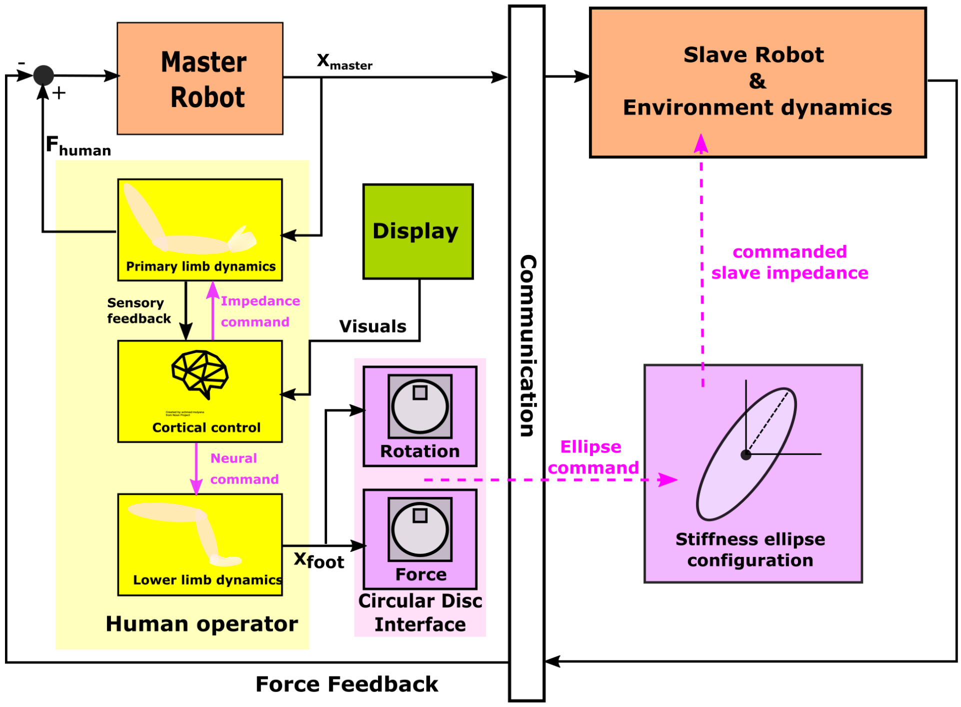
Master Robot
$x_{master}$
Slave Robot & Environment dynamics
-
+
$F_{human}$
Primary limb dynamics
Display
Communication
commanded slave impedance
Sensory feedback
Impedance command
Visuals
Cortical control
Rotation
Ellipse command
Neural command
Stiffness ellipse configuration
Lower limb dynamics
$x_{foot}$
Force
Circular Disc Interface
Human operator
Force Feedback

Figure A.2: Block scheme of the force feedback tele-impedance setup for the Circular disc interface. The Circular disc interface controls the stiffness ellipse configuration, which is commanded as a Cartesian slave impedance of the slave robot located at the end-effector. The slave robot and environment dynamics block is further explained in Fig. A.3

The slave robot and environment dynamics change by the presence of an interaction with the wall or perturbation applied. To clearly define dynamic changes of the slave robot and environment dynamics we divided the dynamics in four different situations:

- Movement in free space
- Interaction with the environment
- Applied force perturbation
- Drill insertion
- Applied position perturbation

### A.2.1. Movement in free space

During the movement in free space, no interaction between end-effector of the slave and the environment will be present. Since we assumed perfect inertia and gravity compensation of the slave, the position and velocity of the slave will follow the reference position and velocity of the master perfectly. Papers present an increase of positional accuracy during reaching tasks if damping will be fed back to the master. However, since we are not interested in the reaching task to the position of insertion of the drill we did not include this. Therefore the relation between reference and slave position and velocity is the following:

$$\boldsymbol{x}_{ref} = \boldsymbol{x}_{slave} \quad and \quad \dot{\boldsymbol{x}}_{ref} = \dot{\boldsymbol{x}}_{slave} \tag{A.1}$$

where $\boldsymbol{x}_{ref}$ and $\boldsymbol{x}_{slave}$ are the reference position of the manipulator and the actual position of the slave. $\dot{\boldsymbol{x}}_{ref}$ and $\dot{\boldsymbol{x}}_{slave}$ are the reference velocity of the manipulator and the actual velocity of the slave.

### A.2.2. Interaction with the wall

When the end-effector of the slave makes contact with the environment, the dynamics of the slave change because the reference position cannot be followed perfectly. This is due to the environment not allowing the slave to move through the wall while the reference position of the master can. Therefore an interaction force will be present calculated by the impedance controller as

$$\boldsymbol{F}_s = \boldsymbol{K}_s(\boldsymbol{x}_{ref} - \boldsymbol{x}_{slave}) - \boldsymbol{D}_s(\dot{\boldsymbol{x}}_{ref} - \dot{\boldsymbol{x}}_{slave}) \tag{A.2}$$

where $\boldsymbol{F}_s$ is the interaction force between end-effector of the slave and environment, $\boldsymbol{K}_s$ the stiffness matrix of the slave and $\boldsymbol{D}_s$ the damping matrix of the slave. The interaction force between slave and environment will be used as haptic feedback signal back to the master to present the operator a feel of the environment during bilateral teleoperation.

### A.2.3. Applied force perturbation

During the finding the hole phase a force perturbation will be applied at the end-effector of the slave. The introduction of a perturbation will include a mass, which will be added to the system. This mass is an environmental mass pushing onto the object. Therefore, an error between the reference position of the master and the actual position of the slave can be present. The dynamics of the slave including the force perturbation are illustrated in Fig. A.3.

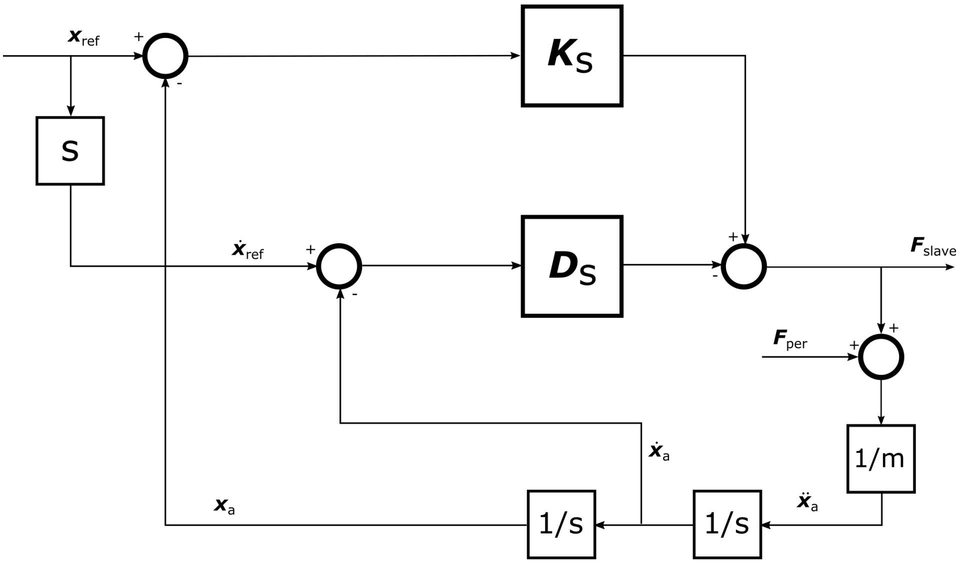

$\boldsymbol{x}_{\text{ref}}$
+
-
S
$\boldsymbol{K}_S$
$\dot{\boldsymbol{x}}_{\text{ref}}$
+
-
$\boldsymbol{D}_S$
+
-
$\boldsymbol{F}_{\text{slave}}$
$\boldsymbol{F}_{\text{per}}$
+
+
1/m
$\dot{\boldsymbol{x}}_{\text{a}}$
$\ddot{\boldsymbol{x}}_{\text{a}}$
$\boldsymbol{x}_{\text{a}}$
1/s
1/s

Figure A.3: Block scheme of the slave and environment of the slave robot and environment dynamics block of Fig. A.2. $\boldsymbol{x}_{ref}$ and $\dot{\boldsymbol{x}}_{ref}$ are the reference position and velocity of the manipulator. $\boldsymbol{F}_{slave}$ is the remote robot force and $\boldsymbol{F}_{per}$ the force perturbation applied on the robot end-effector. $\ddot{\boldsymbol{x}}_a$,$\dot{\boldsymbol{x}}_a$ and $\boldsymbol{x}_a$ are the actual acceleration, velocity and position of the end-effector.

The addition of the force perturbation will be included to the total force feedback to the master console by

$$\boldsymbol{F}_s = \boldsymbol{K}_s(\boldsymbol{x}_{ref} - \boldsymbol{x}_{slave}) - \boldsymbol{D}_s(\dot{\boldsymbol{x}}_{ref} - \dot{\boldsymbol{x}}_{slave}) + \boldsymbol{F}_{per} \tag{A.3}$$

where $\boldsymbol{F}_{per}$ is the force perturbation applied on the end-effector of the slave. The additional mass of the environment introduces an acceleration of the master by

$$\ddot{\boldsymbol{x}}_t = \frac{\boldsymbol{K}_s}{m}(\boldsymbol{x}_{ref} - \boldsymbol{x}_{slave}) - \frac{\boldsymbol{D}_s}{m}(\dot{\boldsymbol{x}}_{ref} - \dot{\boldsymbol{x}}_{slave}) + \frac{\boldsymbol{F}_{per}}{m} \tag{A.4}$$

with m as the additional mass added as a result of the force perturbation and $\ddot{\boldsymbol{x}}_t$ the acceleration of the slave. To calculate the position and velocity of the slave in the following time step we have to integrate the acceleration, which results in the following:

$$\dot{\boldsymbol{x}}_t = \left(\frac{\boldsymbol{K}_s}{m}(\boldsymbol{x}_{ref} - \boldsymbol{x}_{slave}) - \frac{\boldsymbol{D}_s}{m}(\dot{\boldsymbol{x}}_{ref} - \dot{\boldsymbol{x}}_{slave}) + \frac{\boldsymbol{F}_{per}}{m}\right)\Delta t + \dot{\boldsymbol{x}}_{t-1} \tag{A.5}$$

where $\dot{\boldsymbol{x}}_t$ is the velocity of the slave for time step $t$ and $\Delta t$ the interval of time used to calculate the next time instant. The frequency the control algorithm calculates runs on is 100 Hz, therefore $\Delta t$ will always be 0.01. Subsequently, we perform another integration to calculate the position of the slave for the next time step, resulting in the following:

$$\boldsymbol{x}_t = \frac{1}{2}\left(\frac{\boldsymbol{K}_s}{m}(\boldsymbol{x}_{ref} - \boldsymbol{x}_{slave}) - \frac{\boldsymbol{D}_s}{m}(\dot{\boldsymbol{x}}_{ref} - \dot{\boldsymbol{x}}_{slave} + \frac{\boldsymbol{F}_{per}}{m})\right)\Delta t^2 + \dot{\boldsymbol{x}}_{t-1}\Delta t + \boldsymbol{x}_{t-1} \tag{A.6}$$

with $\boldsymbol{x}_t$, the position of the slave for time step $t$. As illustrated in the block diagram of Fig A.3, the position of the slave and interaction force between slave and environment depends on reference position of the controller, slave position, slave stiffness matrix and slave damping matrix.

# B

# Circular disc interface

## B.1. Design requirements

Interfaces controlling a variable impedance for teleoperation are proposed and evaluated in previous literature. Proposed control interfaces and control methods can be distinguished in two categories. First, EMG methods using EMG sensors and markers attached to the operator to estimate the posture of the arm [4, 11, 21]. The estimation of these methods can create a multi degrees of freedom impedance profile located at the end-effector [3, 7]. However, generally long calibration times and knowledge of human anatomy is needed to successfully transfer the impedance profile from the human operator to the manipulator. Furthermore, EMG methods introduce the coupling effect between force-feedback and commanded stiffness [10]. On the other hand, methods using external devices is a much more simplistic approach to control the impedance of the manipulator [20]. Dominantly hand-held devices are used to regulate the impedance in only one degree of freedom [23]. On top of that, handheld devices can obstruct the operator due to an additional device in the hand for example in bimanual teleoperation. Therefore, we decided to combine the two methods to design a interface having the ability to control a multidimensional stiffness ellipse with minimized calibration procedures, without extended knowledge of human anatomy, no introduction of the coupling effect without the use of hands to control the interface.

## B.2. Circular disc interface design

To meet the design requirements, we created the circular disc interface to alter a stiffness ellipse located at the end-effector of a manipulator based on human stiffness ellipse modulation in a 2D plane. Humans can alter the ellipse of their arm by muscle contraction and changing the posture [5, 6]. Consequently, the stiffness ellipse will be rotated and shaped according to task instruction and influences from the environment including perturbations and need for accuracy [2]. Therefore, two signals to rotate and reshape the stiffness ellipse located at the end-effector of a remote manipulator are introduced by the circular disc interface. First, rotation of the stiffness ellipse is controlled by rotation of the circular disc, which is zero order control illustrated in Fig. B.1. The angle disc indicates the direction of the semi-major axis. Secondly, changing the shape of the ellipse is controlled by a force sensor located in the foot pad.

The circular disc interface consists out of 3 main components illustrated in Fig. B.2. First, a robust main frame ensuring high stability and fixation for sensors. The main frame of the device consists out of two steel squares of 350x350x3mm fixed by 10mm diameter bolts in each corner, which are additionally used as legs. Rubber foots are attached to the frame to eliminate the interface from sliding over the floor.

### B.2.1. Rotating disc

The second component is the rotating disc fixed to a rotating shaft through the middle of the main frame. The shaft is attached to the potentiometer, which measures the rotation of the circular disc. The circular disc has a diameter of 250 mm and a thickness of 2mm and the shaft is a 10mm diameter bolt. To constraint the disc to rotation only around the axis of the attached shaft, a carousel bearing is fixed between the circular disc and frame. Movements or rotations in unintended directions are highly constraint by the carousel bearing. The shaft is attached to a potentiometer by a flexible shaft coupler to compensate for alignment errors of

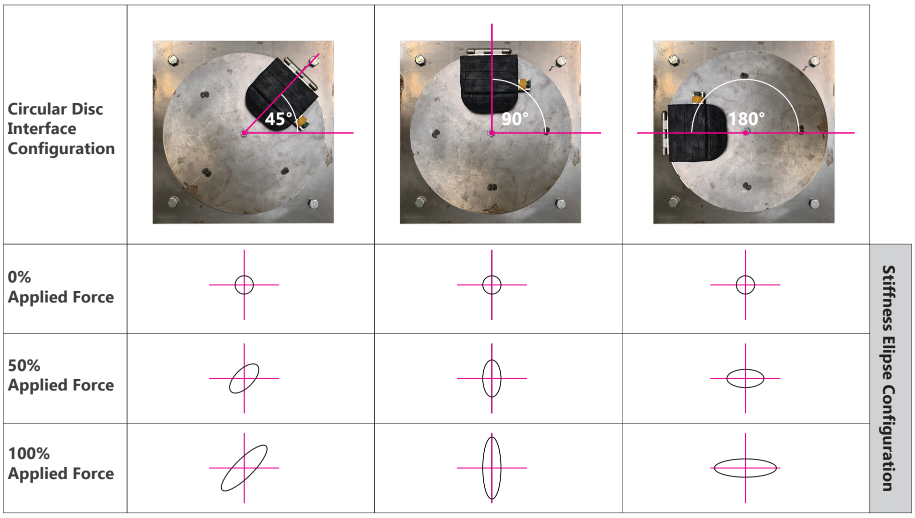
Circular Disc Interface Configuration
45°
90°
180°
0% Applied Force
50% Applied Force
100% Applied Force
Stiffness Ellipse Configuration

Figure B.1: The relation between the configuration of the Circular Disc interface configuration and stiffness ellipse configuration depending on the force exerted on the foot pad and the rotation of the circular disc

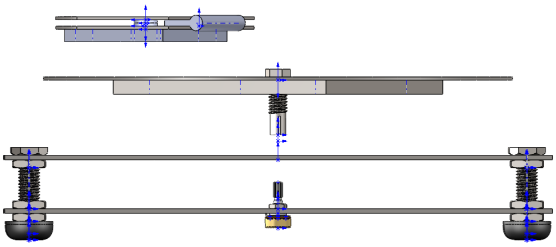

Figure B.2: An exploded view of the circular disc interface showing the three main components. The top component is the foot pad, the middle is the circular disc and the bottom component is the frame.

shaft during rotation. The potentiometer is not rotational constraint, therefore it can rotate around the axis infinitely. However, it can only measure an analog output from 20 to 340 degrees. This is not a problem regarding facilitating every possible configuration of the stiffness ellipse due to the symmetric shape of a stiffness ellipse illustrated in Fig B.1.

### B.2.2. foot pad

The third component is the foot pad attached to the circular disc at 100 mm radius by a 7.5mm diameter carousel bearing to control the rotation of the disc with the foot. The foot pad has the ability to rotate around its own midpoint independently of the circular disc. Therefore, the operator does not have to rotate the foot while rotating the circular disc. A rubber material is attached to the pad to prevent the foot from slipping. A force sensor is located under the foot pad to control the shape of the ellipse. The force sensor is a SingleTact force sensor with 15 mm diameter and a maximum measurable force of 450 Newton [1]. The force sensor has a force resolution of <0.2% of full scale force and a repeatability error of <0.1%. The relationship between force and voltage output has a linear relationship with <0.2% linearity error. The foot pad consists out of a hinge structure to apply all the force exerted by the foot onto the force sensor. The hinge structure consists out of two steel plates fixed to each other by a hinge. The force sensor is attached to the middle of one plate and a force concentration pad with similar diameter as the force sensor is attached to the other plate. As we close the hinge, the force concentration pad will pass all the force by the foot on to the force sensor.

### B.2.3. sensors

The sensors are attached to a National Instruments device illustrated in Fig. B.3. The National Instruments device receives analog signals from the potentiometer and force sensor. The noise of the force sensor is suppressed by a capacitor between the analog input and ground of the national instruments device [19]. Subsequently, the National instruments device will sends the analog signals to the computer via USB connection. Both analog signals are low-pass filtered by a lowpass filter (2nd order Butterworth, cut-off frequency of 5 Hz) determined by pilot studies and [9]. The filter causes minor delays, which are not detrimental for impedance control because high frequency changes of impedance are unnecessary for successfully completing the experimental tasks.

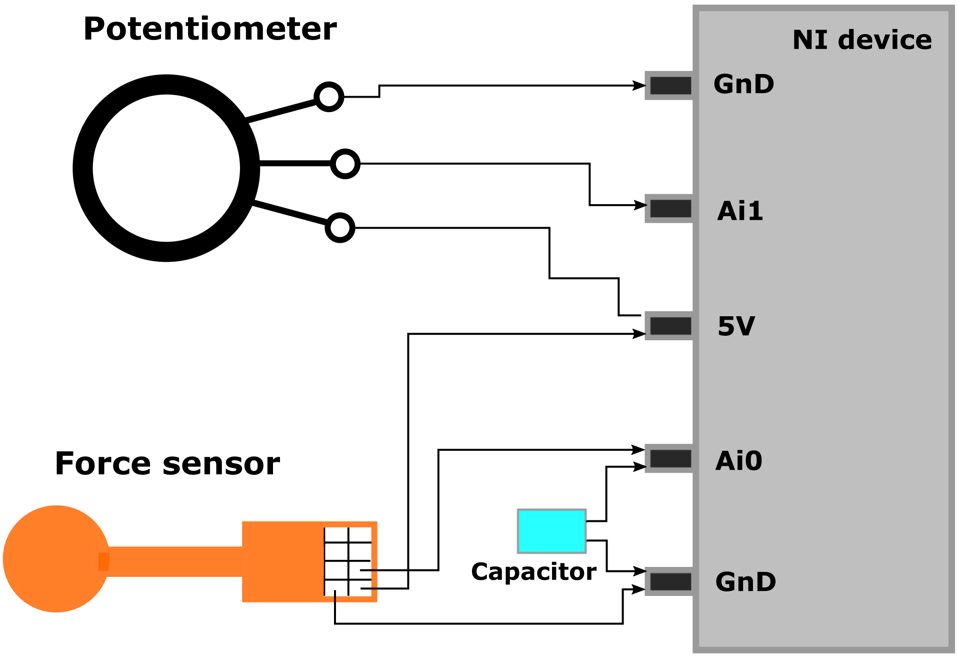

Figure B.3: Electrical connection of the potentiometer and force sensor to the NI device. GnD is the ground, Ai1 and Ai0 are analog inputs and 5V is the voltage output of the National instruments device. A capacitor is placed between Ai0 and GnD to decrease the noise of the force sensor

## B.3. Technical Drawings and HREC device report

In this section the technical drawings of the circular disc interface are presented. First, an overview and exploded view is presented. Subsequently, a technical drawing for every main component is illustrated. At last, the device report approved by the Human Research Ethics Committee of the TU Delft.

Isometric view

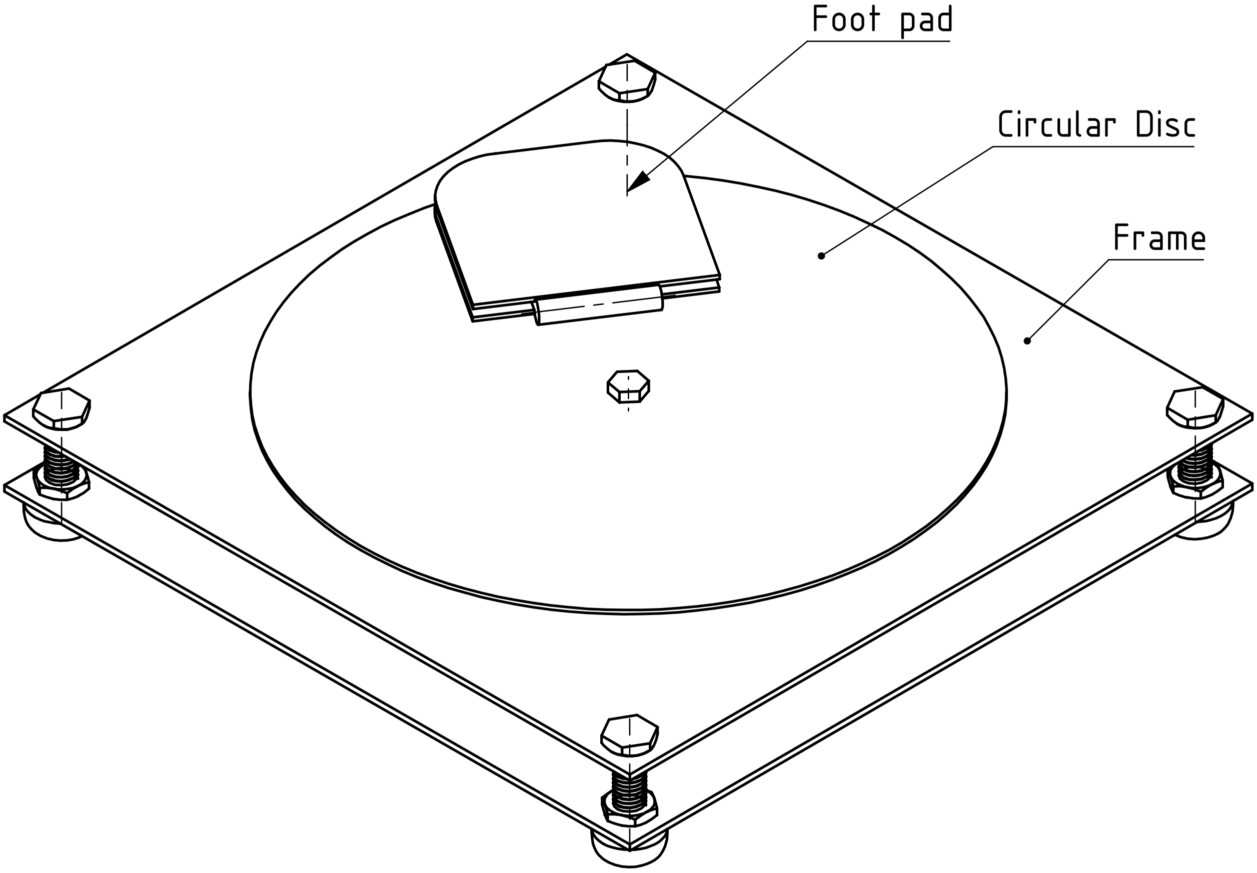
Foot pad
Circular Disc
Frame

Exploded front view

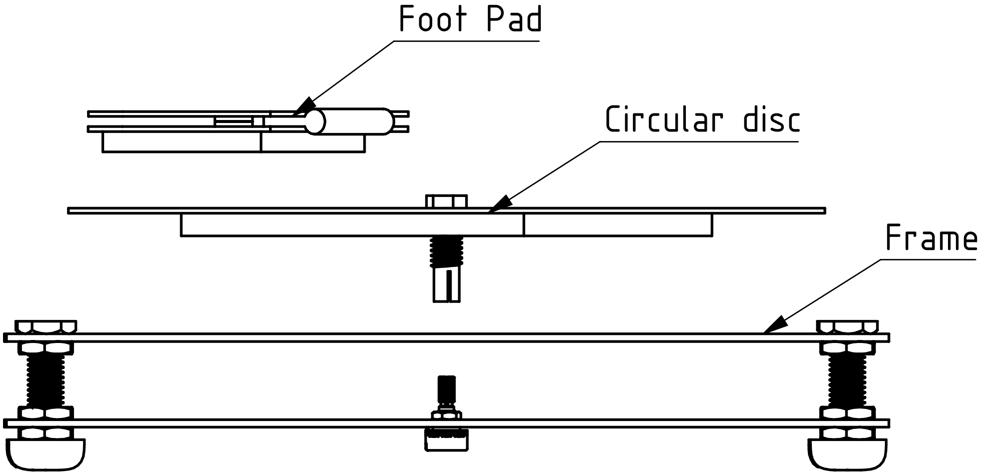
Foot Pad
Circular disc
Frame

| | | | | | |
|---|---|---|---|---|---|
| | units<br>mm | scale<br>1:1 | quantity<br>1 | date<br>18-3-2021 | remark<br><<remarks>> |
| material | | | | mass<br>gr | TU Delft<br>Delft<br>University of<br>Technology |
| author Stijn Klevering 4224329 | | | | group<br><<group>> | |
| name Circular Disc Interface | | | | format<br>A4 | drawing no.<br>1 |

SOLIDWORKS Educational Product. For Instructional Use Only.

Top view

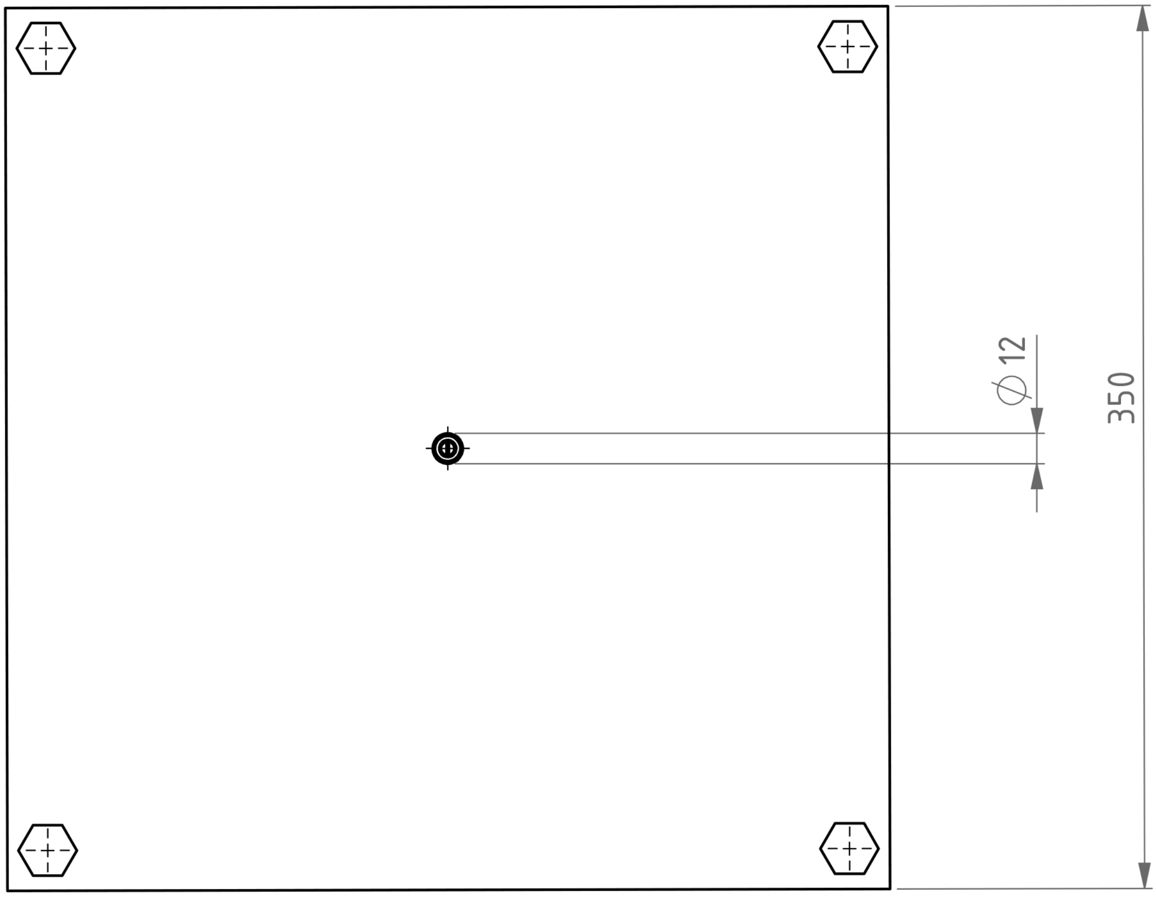

Front view

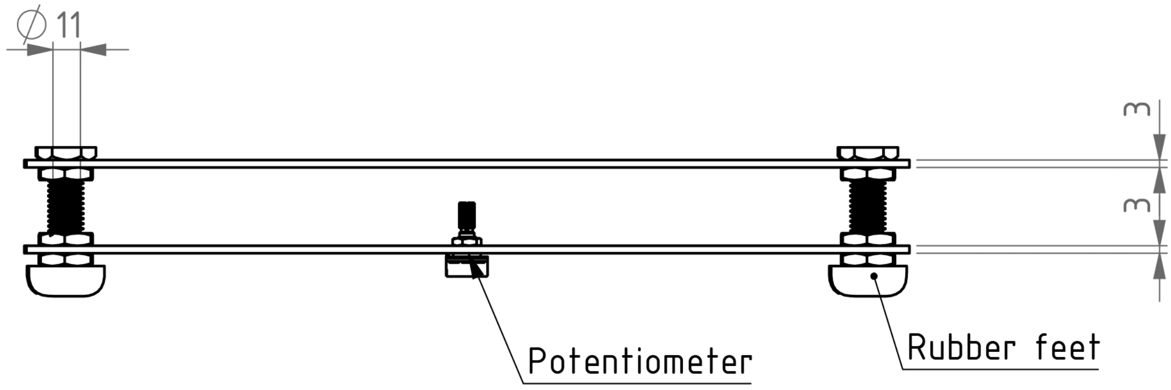
Ø 11
3
3
Potentiometer
Rubber feet

| | | | | | |
|---|---|---|---|---|---|
| | units mm | scale 1:1 | quantity 1 | date 18-3-2021 | remark Frame with potentiometer |
| material | | | | mass gr | TU Delft Delft University of Technology |
| author Stijn Klevering 4224329 | | | | group <<group>> | |
| name **Frame**<br>H:\My Documents\Thesis\Circular disc interface\FootPedal Solidworks - D20\Drawings\ | | | | format A4 | drawing no. 1 |

**SOLIDWORKS Educational Product. For Instructional Use Only.**

Front view

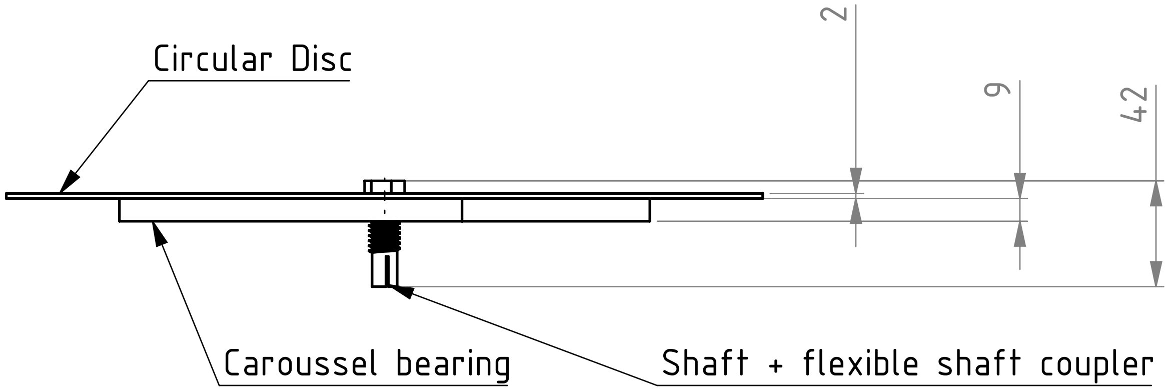
2
9
42
Circular Disc
Caroussel bearing
Shaft + flexible shaft coupler

Bottom view

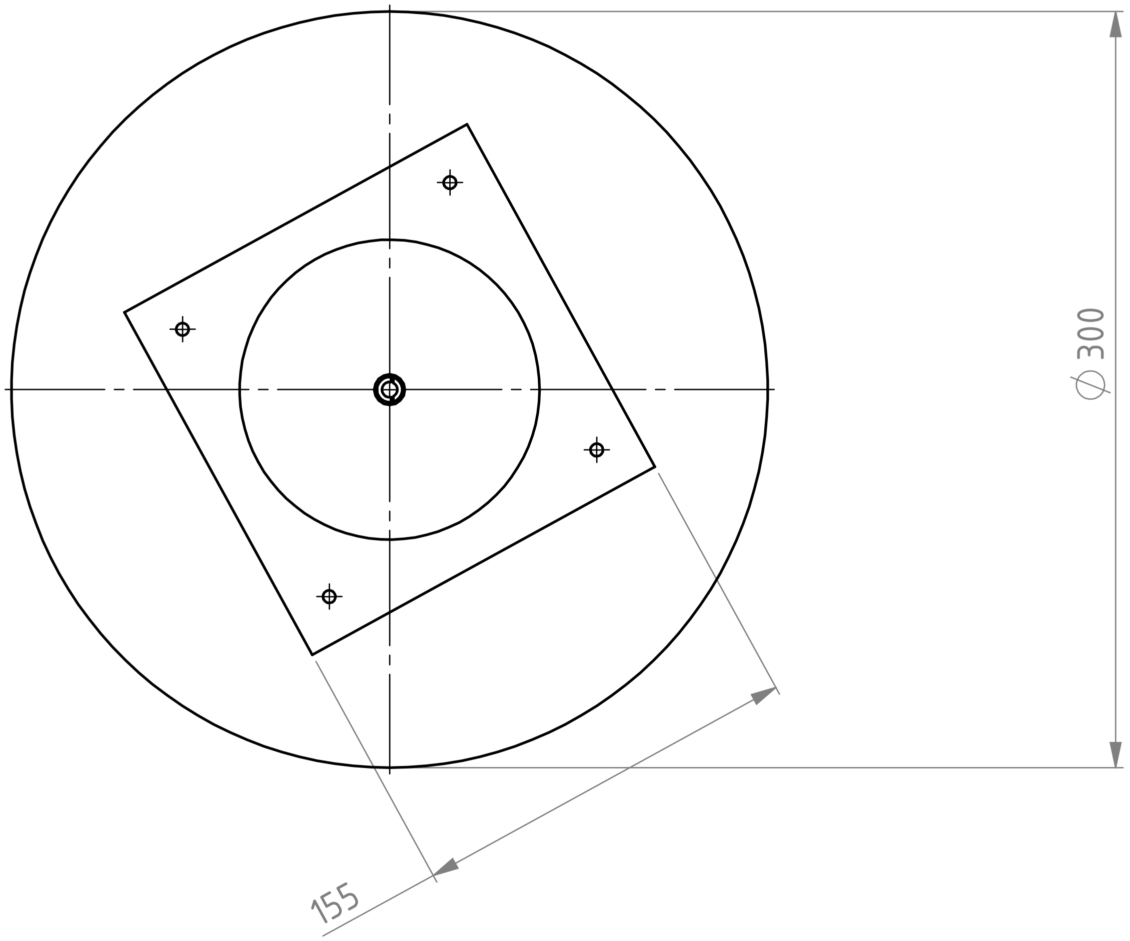

| | | | | |
|---|---|---|---|---|
| units mm | scale 1:1 | quantity 1 | date 18-3-2021 | remark The circular disc with shaft and bearing |
| material | | | mass gr | TU Delft Delft University of Technology |
| author Stijn Klevering 4224329 | | | group <<group>> | |
| name **Circular Disc** | | | format A4 | drawing no. 1 |

H:\My Documents\Thesis\Circular disc interface\FootPedal Solidworks - D20\Drawings\

**SOLIDWORKS Educational Product. For Instructional Use Only.**

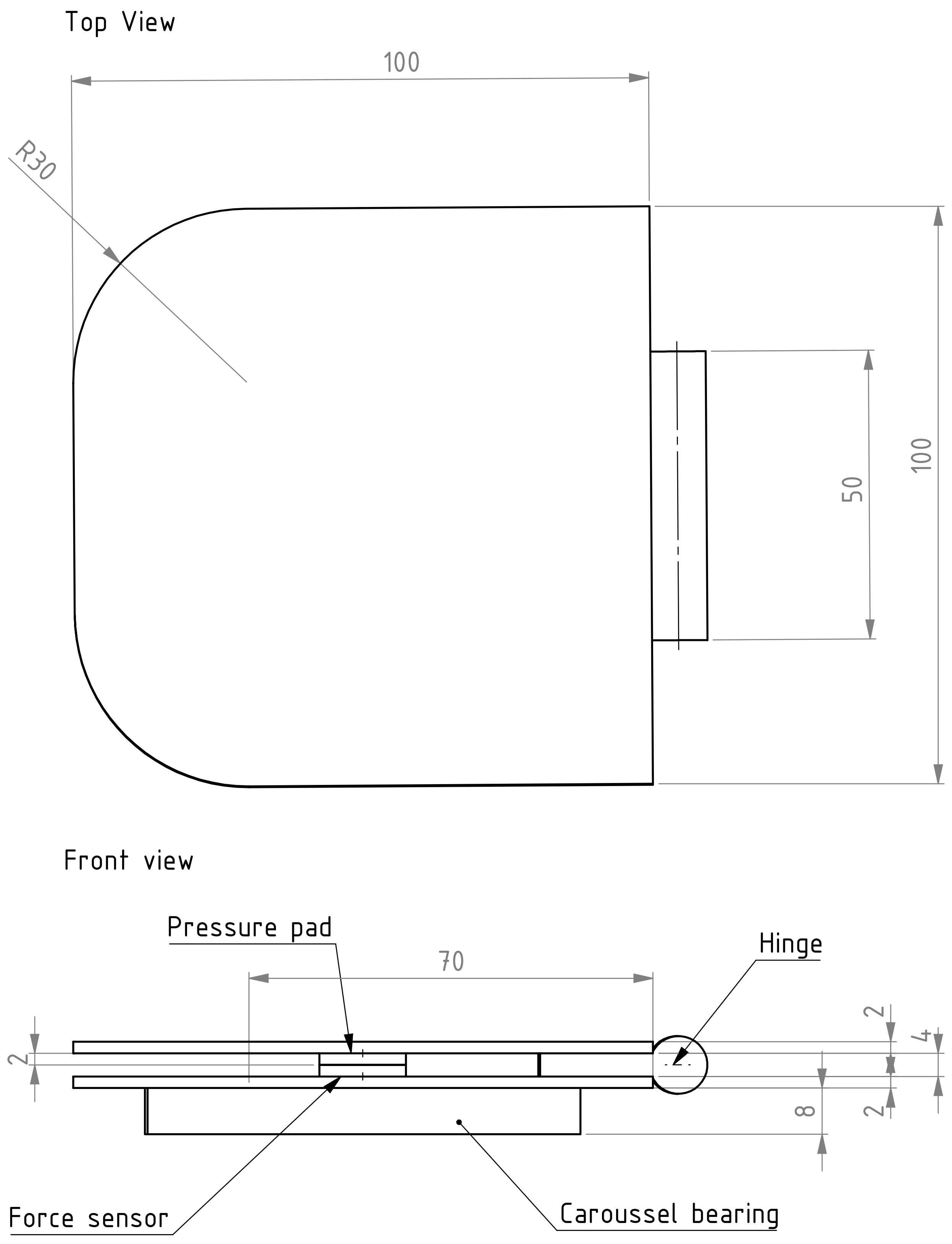
Top View
100
R30
50
100
Front view
Pressure pad
70
Hinge
2
2
4
8
2
Force sensor
Caroussel bearing

| | | | | |
|---|---|---|---|---|
| units mm | scale 1:1 | quantity 1 | date 18-3-2021 | remark <<remarks>> |
| material | | | mass gr | TU Delft<br>Delft University of Technology |
| author Stijn Klevering 4224329 | | | group <<group>> | |

| | | |
|---|---|---|
| name **Foot Pad** | format A4 | drawing no. 1 |

H:\My Documents\Thesis\Circular disc interface\FootPedal Solidworks - D20\Drawings\

**SOLIDWORKS Educational Product. For Instructional Use Only.**

# Delft University of Technology
# INSPECTION REPORT FOR DEVICES TO BE USED IN CONNECTION WITH HUMAN SUBJECT RESEARCH

This report should be completed for every experimental device that is to be used in interaction with humans and that is not CE certified or used in a setting where the CE certification no longer applies[1].

The first part of the report has to be completed by the researcher and/or a responsible technician.

Then, the safety officer (Heath, Security and Environment advisor) of the faculty responsible for the device has to inspect the device and fill in the second part of this form. An actual list of safety-officers is provided on this webpage.

Note that in addition to this, all experiments that involve human subjects have to be approved by the Human Research Ethics Committee of TU Delft. Information on ethics topics, including the application process, is provided on the HREC website.

**Device identification (name, location): Circular Disc Interface, Cognitive Robotics lab 3ME, Delft**

**Configurations inspected[2]: N.A.**

**Type of experiment to be carried out on the device:[3] Virtual impedance control during teleoperation**

**Name(s) of applicants(s):** Stijn Klevering

**Job title(s) of applicants(s):** MSc graduate student

(Please note that the inspection report should be filled in by a TU Delft employee. In case of a BSc/MSc thesis project, the responsible supervisor has to fill in and sign the inspection report.)

**Date: 24/09/2020**

**Signature(s):**

---

[1] Modified, altered, used for a purpose not reasonably foreseen in the CE certification

[2] If the devices can be used in multiple configurations, otherwise insert NA

[3] e.g. driving, flying, VR navigation, physical exercise, ...

## Setup summary

*Please provide a brief description of the experimental device (functions and components) and the setup in which context it supposed to be used. Please document with pictures where necessary.*

*More elaborate descriptions should be added as an appendix (see below).*

The device is a controller to alter an ellipse shaped impedance profile of a virtual object operated by the foot. The device consists out of two variable outputs: Circular disc rotation by a potentiometer and measurement of the force exerted by the foot onto the device (Appendix).
The operator rotates the circular disc with the foot to rotate the virtual stiffness ellipse. Simultaneously, the operator has the possibility to press on the footpad to alter the shape of the virtual stiffness ellipse. This method results in a human-like variable impedance of a virtual end-effector of a robotic arm to conduct various dynamic virtual tasks.
The circular disc interface consists out of 3 separate components. First the main frame with a rubber base, ensuring high stability, eliminating sliding over the floor and fixation of the potentiometer. The second component is a rotating disc fixed to a rotating shaft. The shaft is attached to the rotating part of the potentiometer, therefore the potentiometer measures the angle of rotation of the circular disc. The third component is a footpad attached to the circular disc to be able to rotate the disc with the foot. The operator does not have to rotate the foot while rotating the circular disc due to the ability of rotation of the footpad around its own midpoint.
The circular disc of 250 mm diameter rotates around an axis stabilized by a 150mm carrousel bearing and the main frame of the device (two steel squares of 350x350x3mm fixed by a 10mm diameter bolt in each corner, see appendix). Carrousel bearing only allow rotation around its axis. Movements or rotations in unintended directions are highly constraint while still giving the ability to rotate around the intended axis without effort.
The shaft is attached to a potentiometer by a flexible shaft coupler to compensate for alignment errors of the axis during rotation. The potentiometer can infinitely rotate around its axis. However, it can only measure an analog output from 20 degrees to 340 degrees. The potentiometer is attached to a National Instrument device to send the real-time data to the computer.
Furthermore, the footpad is attached to the circular disc interface at 100 mm radius by a 7,5mm diameter carrousel bearing to enable rotating the foot while rotating the disc. The footpad consists out of a rubber plateau to support the foot and a hinge structure to be able to concentrate the force exerted on the foot pedal to the force sensor. The force sensor (max 450N) is connected to the same National Instrument device as the potentiometer.

**Risk checklist**

Please fill in the following checklist and consider these hazards that are typically present in many research setups. If a hazard is present, please describe how it is dealt with.

Also, mention any other hazards that are present.

| Hazard type | Present | Hazard source | Mitigation measures |
|---|---|---|---|
| Mechanical (sharp edges, moving equipment, etc.) | Yes | A rotating disc controlled by the foot of the participant.<br>Movement of the device. | The device has weight of +/- 6 Kg and placed on the ground. The rotating disc is solid made of steel plate 2mm thick supported by a strong frame of 300x300x3mm plates fastened by 10mm diameter bolts (see Appendix). Edges softened by filing.<br>To prevent sliding on the ground, the device has rubber foots and a rubber attached on the pad to control the device. |
| Electrical | Yes | 5V output from National Instruments device. | The device has rubber foots and a rubber attached on the pad to control the device, thus the participant does not touch any conducting materials.<br>Furthermore, the current is too low to give any harm. |
| Structural failure | No | | |
| Touch Temperature | No | | |
| Electromagnetic radiation | No | | |
| Ionizing radiation | No | | |
| (Near-)optical radiation (lasers, IR-, UV-, bright visible light sources) | No | | |
| Noise exposure | No | | |
| Materials (flammability, offgassing, etc.) | No | | |
| Chemical processes | No | | |
| Fall risk | No | | |
| *Other:* | | | |
| *Other:* | | | |
| *Other:* | | | |

# C

# Ideal stiffness ellipse strategy

Tasks conducted by human limbs generate an optimal stiffness strategy depending on task instruction, environment and uncertainties within that environment [2, 18]. Multiple studies have been done on how humans tend to change their limb impedance to the dependencies [6, 12, 14]. The human limb stiffness is produced by excitatory or inhibitory muscle Golgi tendon force feedback, co-contraction, muscle spindle feedback and posture [18]. The Golgi tendon lies at proximal and distal ends of the muscle fibers into the tendons of skeletal muscles. It provides the ability to measure the force in the muscles used for spinal reflexes and cerebellar regulation of movement. Co-contraction is activated by intentionally contracting both the agonist and antagonist muscles to increase the stiffness of the human arm. Co-contraction ensures for time delays like proprioceptive feedback but costs more energy. Muscle spindle feedback are proprioceptors that detect changes in the length of muscles providing reflexive motor control and positional information to the central nervous system. Furthermore, the human limb tends to adjust the posture to adjust the impedance and become more energy efficient [14].

Task instruction, environment and uncertainties of the environment highly influence the four control aspects of the human limb and therefore the human limb stiffness. To determine the strategies humans use to adapt to situations we look into task instructions (position tasks and force tasks) and environmental perturbations applied (force and position perturbations).

A position task was conducted by Buzzi et al. 2017 where the participant had to follow a trajectory with changing curvature [6]. As the curvature increased, the stiffness of the limb significantly increased. This indicates that as a trajectory task difficulty increases the stiffness of the limb increases to keep on the reference trajectory. Gomi et al. 1998 studied the controllability and spatial characteristics of the human arm during force interactions in various directions during posture maintenance and force regulation tasks supported by Flash et al. 1990 [12, 14]. They found that the arm posture affects the controllability of orientation and shape of a stiffness ellipse located at the end-point of the arm. Therefore, the human tend to change posture to alter the stiffness profile of the arm. Mugge et al. 2010 studied the contributions of muscle force feedback, co-contraction and muscle spindle activity to performance during position tasks, force tasks and relaxation tasks while perturbations where applied [18]. During position tasks, participants resisted perturbations by becoming more stiff. Furthermore, force tasks induced the participant to become more compliant. Abbink et al. 2007 supports this statement in an experimental study showing substantial modifiable human endpoint dynamics while interacting with a haptic manipulator [2].

Literature generally describes the human arm stiffness located at the endpoint as a stiffness ellipse. Since we are controlling a stiffness ellipse located at the end-effector of a robotic manipulator with the circular disc interface during the experiment, we can estimate the ideal stiffness ellipse strategy during the finding the hole phase and the drill insertion phase depending on task instruction, environment orientation and perturbation. The full experimental method of the finding the hole phase and drill insertion phase are further explained in appendix D.

During the finding the hole phase the operator is instructed to hold a reference force at the wall in insertion direction and hold a reference position perpendicular to insertion direction illustrated in Fig. C.1. During the task a force perturbation is applied perpendicular to insertion direction of the drill. Humans are more accurate in holding a reference force when being more compliant to the environment. Therefore, the ideal stiffness profile of the end-effector in insertion direction is a low stiffness. Furthermore, humans increase their performance regarding positional accuracy by becoming more stiff, especially when force perturbations are applied. Therefore, a high stiffness perpendicular to insertion direction is desired to hold the reference position of the end-effector. To achieve this stiffness strategy, the participant has to rotate the circular disc interface so that the direction of the semi-major axis of the ellipse is directed perpendicular to insertion direction. Subsequently, the participant has to increase the stiffness in the direction of the semi-major axis by applying force on the foot pad of the circular disc interface.

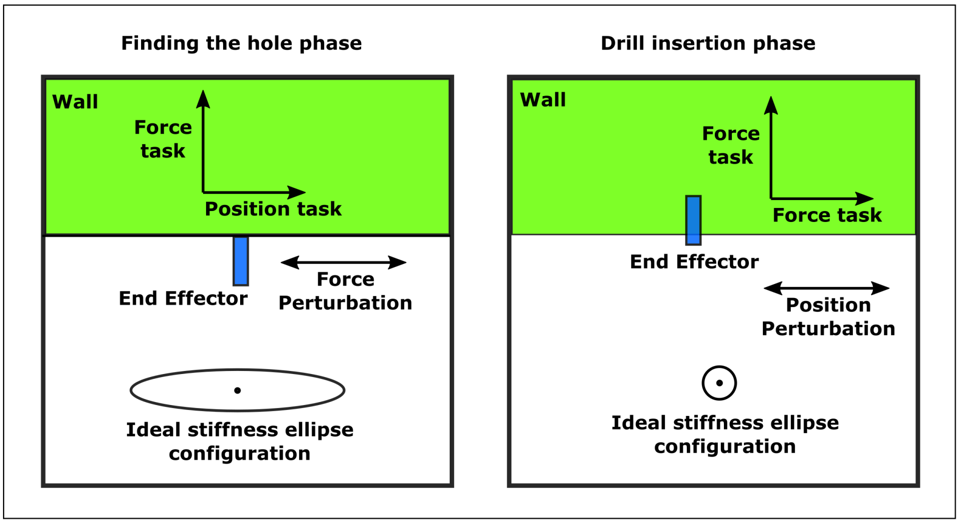
Finding the hole phase
Wall
Force task
Position task
End Effector
Force Perturbation
Ideal stiffness ellipse configuration
Drill insertion phase
Wall
Force task
Force task
End Effector
Position Perturbation
Ideal stiffness ellipse configuration

Figure C.1: The ideal stiffness ellipse strategy during a drilling task with respect to environment, task instruction and perturbation direction. The ideal stiffness ellipse configuration is depicted per phase of the drilling task.

During the drill insertion phase the operator is instructed to minimize the forces perpendicular to insertion direction in order to prevent damaging the end effector or environment, which translates to a force task illustrated in Fig. C.1. On top of that, a position perturbation is applied at the environment. Therefore, the operator has to move with the position perturbation to minimize the forces. This has the consequence that the operator wants to decrease the stiffness perpendicular to insertion direction. Furthermore, the operator is instructed to hold a reference force in insertion direction. During the insertion task, the drill will be inserted in the environment. Therefore, the operator has to perform a force task in insertion direction and has to decrease the stiffness to have better force control. To achieve a low stiffness in both directions, the operator should simply not apply force on the foot pad of the circular disc interface. The stiffness ellipse configuration will simply be a circle of minimum stiffness, therefore any rotation of the stiffness ellipse will not have influence on the stiffness ellipse configuration.

# D

# Experiment methods

This appendix is used to incorporate material to support the experiment methods in the scientific paper, which would distract from the text.

## D.1. Experiment design

To test the hypothesis for the circular disc interface control method, we design a teleoperation drilling task in a two dimensional plane. The drilling task was divided in a finding the hole task and a drill insertion task. A force perturbation was applied on the end-effector during the finding the hole task perpendicular to insertion direction and a position perturbation was applied on the environment during the drill insertion task.

### D.1.1. Independent variables

We used three independent variables to asses the performance of the variable impedance controlled by the circular disc interface including force feedback setting (unilateral and bilateral), impedance mode (high uniform impedance, low uniform impedance and variable impedance). The variable impedance was controlled by the circular disc interface. The low uniform impedance consisted out of a minimum stiffness of 200N/m and the high uniform impedance consisted out of a maximum stiffness of 1500 N/m determined by pilots. Furthermore, the environment was rotated between trials to induce a variable configuration of the ideal stiffness ellipse illustrated in Fig. D.1.

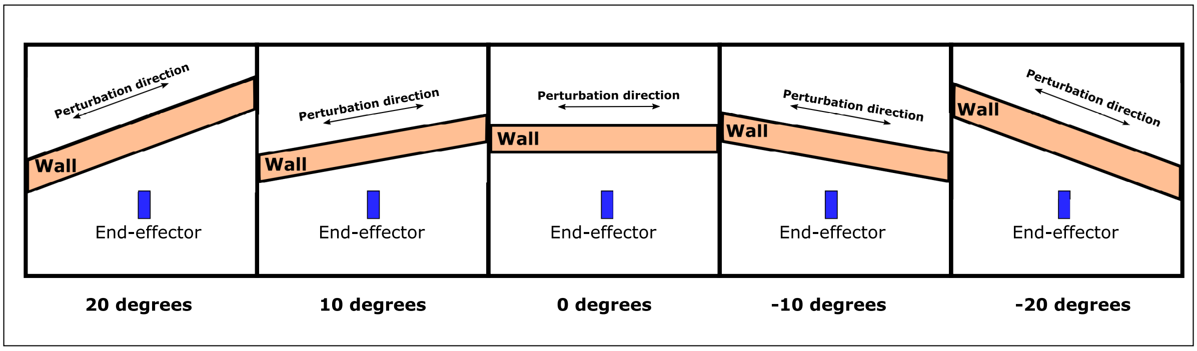
Perturbation direction
Wall
End-effector
20 degrees
Perturbation direction
Wall
End-effector
10 degrees
Perturbation direction
Wall
End-effector
0 degrees
Perturbation direction
Wall
End-effector
-10 degrees
Perturbation direction
Wall
End-effector
-20 degrees

Figure D.1: A visualization of the orientation of the wall applied between trials (-20, -10, 0, 10, 20 degrees). Additionally, the perturbation direction is visualized. The direction of the perturbation depends on rotation of the environment.

### D.1.2. Drilling task

To complete the drilling task the participant had to complete the finding the hole and drill insertion phase. The phases contained constraints for completion. Fig. D.2 visualizes the drilling task for time instances.

1. The experiment is not activated (red wall indication), therefore the end-effector will not move on the monitor and the master will not receive any feedback.

2. The master is pulled back, which activates the experiment and the start of the finding the hole phase indicated by a green wall.
3. The end-effector touches the wall and will activate the force perturbation on the end-effector. In this stage the participant has to hold a reference force parallel to insertion direction and hold a position reference perpendicular to insertion direction for 10 seconds.
4. The 10 seconds are passed. The experiment is deactivated again until the end-effector is pulled away from the wall.
5. The end-effector is pulled away from the wall activating the drill insertion phase.
6. The end-effector touches the wall and can be inserted into the wall.
7. After 1mm insertion of the end-effector in the wall the position perturbation is applied on the wall, which lets the wall move perpendicular to insertion direction.
8. The end-effector is inserted in the wall. The red color indicates again the completion.

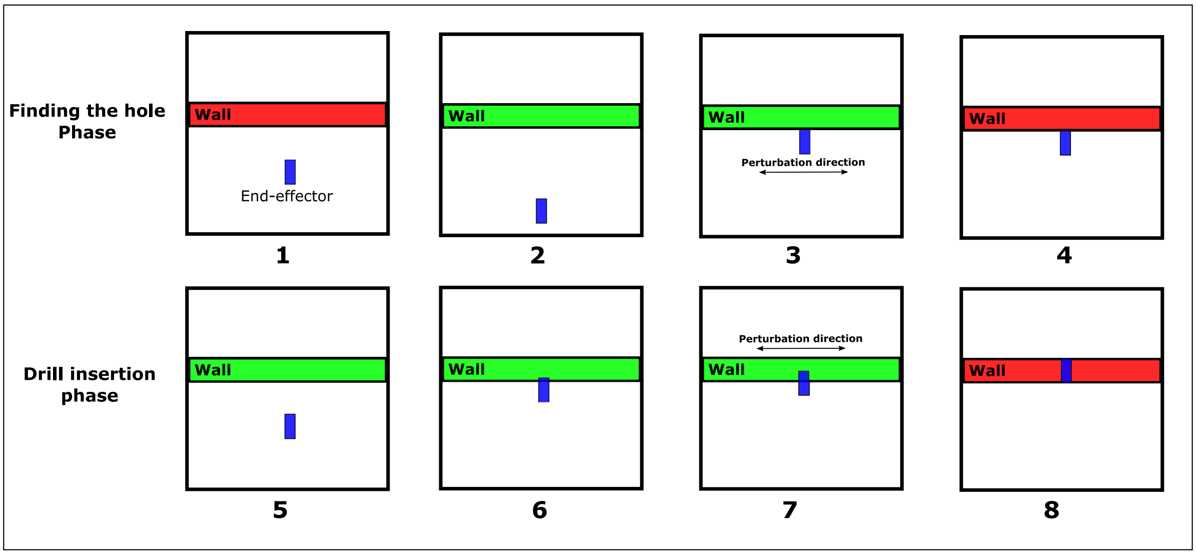

Figure D.2: A visualization of the drilling task for the finding the hole phase and drill insertion phase. The numbers 1-8 indicate time instances within the task important for successful task execution explained in the text.

### D.1.3. Drill insertion

During the drill insertion phase of the experiment, the operator has to insert the drill through the wall at the designated location further explained in appendix E.4. The drill insertion velocity depends on the force exerted on the wall illustrated in Fig. D.3. The drilling force introduces a insertion velocity altering the depth of the hole in the wall. The velocity the depth of the hole has a linear relationship with the force exerted on the wall from 9 to 11 Newtons. This is decided due to an optimal drilling force of 10 N, which is tracked by the operator and pilot study.

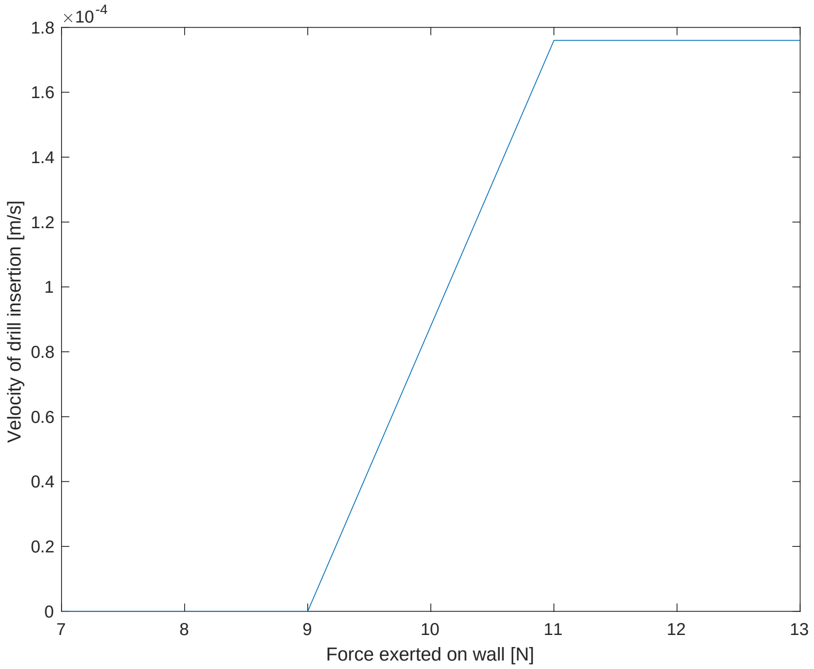

Figure D.3: A visualization of the drilling task for the finding the hole phase and drill insertion phase. The numbers 1-8 indicate time instances within the task important for successful task execution explained in the text.

### D.1.4. Randomization of trials

The sessions were randomized within the groups. We first randomized the force feedback setting. Within the force feedback setting, we randomized the impedance mode. This resulted in the randomization order shown in table D.1. Additionally, the rotations of the environment are randomized within the session.

Table D.1: Randomization order of the sessions for all participants. U is unilateral, B is bilateral, H is high uniform impedance, L is low uniform impedance and V =is variable impedance

| | Session 1 | Session 2 | Session 3 | Session 4 | Session 5 | Session 6 |
|---|---|---|---|---|---|---|
| P1 | UH | UL | UV | BH | BL | BV |
| P2 | UL | UV | UH | BL | BV | BH |
| P3 | UV | UH | UL | BV | BH | BL |
| P4 | BH | BL | BV | UH | UL | UV |
| P5 | BL | BV | BH | UL | UV | UH |
| P6 | BV | BH | BL | UV | UH | UL |
| P7 | UL | UH | UV | BL | BH | BV |
| P8 | UH | UV | UL | BH | BV | BL |
| P9 | UV | UL | UH | BV | BL | BH |
| P10 | BL | BH | BV | UL | UH | UV |
| P11 | BH | BV | BL | UH | UV | UL |
| P12 | BV | BL | BH | UV | UL | UH |

### D.1.5. Perturbation design

Force perturbation

The force perturbation is applied on the end-effector of the virtual manipulator during the finding the hole task, which is in parallel direction of the wall. In other words, perpendicular to insertion direction of the end-effector. Notice that the direction of the force perturbation depends on the rotation of the environment.

We wanted to generate the force perturbation with a multi-sine based on square waves. However, after the experiments were done, we found out that a single sine perturbation was activated. The single sine perturbation was used in pre-trials to confirm if the perturbation was working. Therefore, the applied force perturbation was

$$F_{per} = 3sin(5t) \tag{D.1}$$

with $F_{per}$ the perturbation force and $t$ the time instant of the phase. The perturbation has a amplitude of 3N with a frequency of 0.8 Hz illustrated in Fig. D.4. Furthermore, the force perturbation will add a mass of 1Kg to the system due to the slave and environment dynamics explained in appendix A.

The position perturbation applied is based on square wave perturbation. A square wave perturbation alternates the amplitude between fixed minimum and maximum values, which is represented as Fourier series of sinuses. The transitions between minimum and maximum values are instantaneous for ideal square waves. We intentionally made the square wave imperfect to create an unpredictable perturbation. This was done by using a finite Fourier series of four harmonics and adjusting the amplitude of the individual sinuses.

The wave perturbation is in the form of

$$x_{per} = \frac{0.1}{\pi} sin(\frac{\pi}{3} t) + \frac{0.1}{5\pi} sin(\frac{5\pi}{3} t) + \frac{0.1}{7\pi} sin(\frac{7\pi}{3} t) + \frac{0.4}{9\pi} sin(\frac{9\pi}{3}) \tag{D.2}$$

which is a multi-sine consisting out of sinuses with the frequencies: 0.17Hz, 0.83Hz, 1.17Hz, 1.5Hz. With amplitudes of 0.0318m, 0.0064m, 0.0045m and 0.0141m, respectively. The multisine is illustrated in Fig. D.5.

The position perturbation is applied on the environment. Therefore, the perturbation moves the environment and will not add an additional mass to the system like the force perturbation does. During the position perturbation, the slave is drilling the hole in the environment. Therefore, the slave is constraint by the environment and follows the position perturbation of the environment. The constraints of the environment and position perturbation introduce an error between reference position of the master and position of the slave.

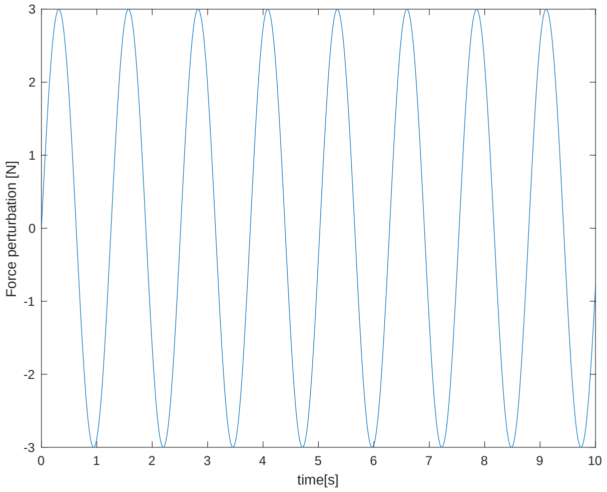

Figure D.4: The force perturbation applied on the end-effector during the finding the hole task.

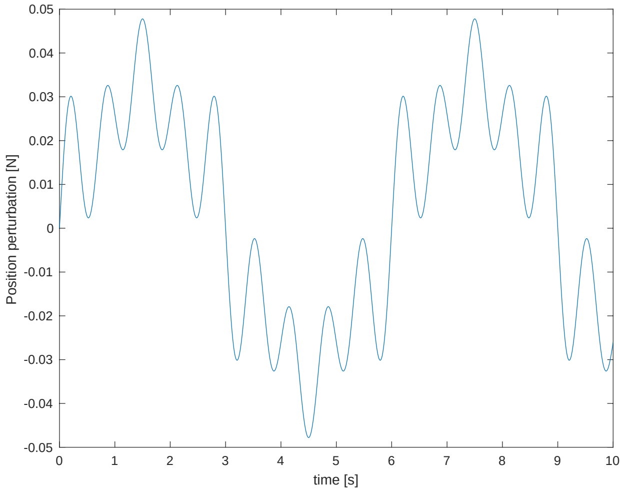

Figure D.5: The position perturbation applied on the end-effector during the finding the hole task.

## D.2. Matlab and C++ code

The Matlab and C++ code are connected through a UDP connection sending data for visualization and data acquisition in a frequency of 100Hz illustrated in Fig. D.6. The C++ code receives signals from the master device and circular disc interface. The receiver of the signals from the circular disc interface through the NI-device is runned separately from the main code.

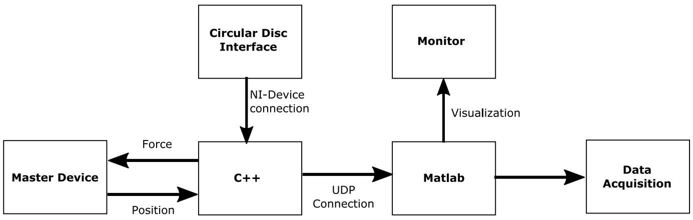
Circular Disc Interface
Monitor
NI-Device connection
Visualization
Force
Master Device
C++
Matlab
Data Acquisition
Position
UDP Connection

Figure D.6: An overview of the Matlab and C++ environments including connections from hardware. The Matlab and C++ environment are both on the same computer connected through a local UDP connection

The type of experiment can be changed by procedure number. The following numbers represent a procedure:

1. Push against a wall with constant stiffness.
2. Push against a wall with variable 1 degrees of freedom stiffness.
3. Push against a wall with a visualized variable stiffness ellipse.
4. The experiment without perturbations
5. The experiment with low uniform impedance
6. The experiment with high uniform impedance
7. The experiment with variable stiffness

The MATLAB code visualizes the experiment on the monitor and saves the data in the designated folder by a Simulink model.

## D.3. Understanding and training

The participant needs a thorough and clear explanation about teleoperation and tele-impedance commanding method. Furthermore, a clear understanding is needed how the experiment is shaped and what the goal of the participant is during the different phases of the drilling task. We conducted a understanding and training session before the experiment since we do not expect the participant to have extensive knowledge about tele-impedance control.

### D.3.1. Understanding session

The understanding session was conducted to inform the participant about teleoperation with and without force feedback, tele-impedance and the control by the circular disc interface. The explanation is itemized with instructions for the observer and instructions how to explain it, which have to be conducted.

Teleoperation

- Ask if the participant is familiar to teleoperation and explain the concept of teleoperation.
    - Teleoperation is a method that allows the human to operate a remote robotic arm at a distance trough a master interface (point at the Sigma.7 device). The operator controls the remote robotic arm movements with the movements of their own arm. In essence the interface measures the motion of the operators hand, which is sent as a commanded motion to the robot.
- Conduct a press against a wall task without force feedback and high uniform impedance mode and note that the remote robot is simulated in the virtual remote environment.
- Explain the participant about force feedback in the teleoperation system.
    - The master can also reproduce the forces that the remote robot feels, so that the operator knows what is happening at the remote site. This is called force feedback.
- Conduct a press against a wall task with force feedback.

Tele-impedance

- Explain the concept of tele-impedance.
    - This master interface can only control the robot motion. On the other hand, the human arm can become stiffer and compliant in different directions (show on your own arm). For example, when we are interacting with a delicate object like glass or human tissue in surgery, it is important to be soft or compliant in order not to damage it. On the other hand, if we want to hold our posture, we stiffen up our arm to counter any interaction forces.
- Conduct a press against a wall task with force feedback and low uniform impedance mode and note the differences between high uniform impedance and low uniform impedance.
- Explain a dynamical variable stiffness
    - With tele-impedance we can control the stiffness of the manipulator in real time and therefore adjust it according to the task or environment.
- Conduct a press against a wall task with force feedback and 1 degrees of freedom variable impedance with force feedback and without force feedback. Let the participant press against the wall and change the impedance by pressing on the foot pad of the circular disc interface.

Circular Disc Interface

- Explain the Circular disc interface
    - To enable the operator to control the robot stiffness we developed a new interface (point at Circular disc interface). The directions in which the robot arm is stiff or soft are represented by the stiffness ellipsoid. In the long axis the stiffness of the robot is variable and in the short axis, the robot is compliant/soft. We can use the developed interface to control the rotation of the ellipsoid by rotating the disc and its shape by pressing on the foot pad (show how you change the ellipsoid).
- Conduct a press against the wall task without perturbations, with and without force feedback and the two dimensional variable stiffness which will be visualized on the monitor at the end-effector.

Drilling task

- Explain the drilling task
  - We have a task where you will have to use the simulated robot to drill a hole into a wall. This task consists of two phases. First, finding the hole on a specific location on the wall surface. During the phase the goal is to hold a reference force (visualized) and the reference position at the drill location. Second, when the initial hole is created, insert a drill into the hole and drill through the wall. The goal is to minimize the force perpendicular to insertion direction to ensure the drill and wall will not be damaged and hold a reference force in the drilling direction.
- Conduct a drilling task with and without force feedback and the two dimensional variable stiffness but without perturbations. Explain the objects visualized on the monitor. - Explain perturbations applied during the task
  - But in real task when you starting making the hole on a surface, there will be a perturbation due to the drill rotating around the surface. The goal is to hold your position while the perturbation is applied. In both phases the task is to maintain the optimal drilling force perpendicular to the wall surface. When you get into the hole the environment locks the drill so it stops moving. However, in some cases, when the environment or robot base is not stable, it might be moving (e.g., deep sea maintenance where wave and currents might affect the operation). To minimize the probability for damaging the drill or environment you have to minimize the forces perpendicular to insertion direction when the drill is locked into the environment.
- Conduct a drilling task with perturbations with low and high uniform impedance mode. Point out the differences regarding performance for both phases and discuss with the participant what the ideal stiffness ellipse strategy will be.
- Explain the stiffness ellipse strategy
  - Stiff in the direction of perturbation (parallel to the surface) in the first phase to be precise in making the initial hole, and complaint in the direction of perturbation (parallel to the wall surface) in the second phase to minimize the parallel force in order not to break the drill or damage the environment. Since your task is also to maintain an optimal force in the drilling direction, it is useful to be compliant in that direction because you can control it more precisely with the commanded reference position.

Experiment procedure

- We will do the task with and without force feedback. So in one case you will be able to feel the forces between the robot and environment, and in the other you will not and will only control the motion/stiffness.
- There will also be three different types of stiffnesses. One where you will control the stiffness with the developed interface and one where the stiffness will be constant and preset at high and low uniform stiffness.
- The order of the force feedback setting will be randomized. Within the force feedback setting, the impedance mode will be randomized.
- Furthermore, different trials will have different orientations of the wall, so you will need to adjust the drill orientation and stiffness ellipsoid strategy to the wall. The orientations will also be randomized per session.

Training session

During the training session the participant conducted the drilling task with perturbations for every force feedback setting and impedance condition. The rotation of the environment was randomized per session. During the training session, the observer can give additional information about the stiffness ellipse strategy and answer any question regarding the environment and goals of the participant.

## D.4. Informed Consent

On the following two pages, the informed consent form is presented.

# Informed consent form

**Title of Research**

Tele-impedance based control architecture based on human arm stiffness ellipse modulation.

**Date** 18/01/2020

Dear Sir / Madam,

You have been asked to participate in a research study titled Tele-impedance based control architecture based on human arm stiffness ellipse modulation. This study is being done by Stijn Klevering from the TU Delft. In this letter you will find information about the research. If you have any questions, please contact the persons listed at the bottom of this letter.

**Background of the research**

During teleoperation a human is able to conduct tasks at a remote location through a controller and a robotic arm. Teleoperation is nowadays extensively used to imbed the adaptability of the operator in unstructured and unpredictable environments such as robotic surgery, assembly, deep-sea and space exploration, first responder applications and military applications. Despite of the advantages teleoperation brings, it brings adverse consequences like the inability to feel structures, deteriorated 3D visual feedback, delays and the possibility for damaging tool and environment.
To deal with the disadvantages, a control architecture called tele-impedance has been introduced. Tele-impedance gives the operator the ability to dynamically alter the stiffness of the robotic arm in real-time according to compensate for uncertainties in task execution and environment. Specifically bimanual teleoperation, teleoperation with two robotic arms, has to deal with unstructured and unpredictable environments. However, there has been no method introduced to implement tele-impedance in bimanual teleoperation executing challenging tasks.

**Purpose of the research**

The purpose of this research study is to introduce a tele-impedance control architecture for bimanual teleoperation using human arm stiffness ellipse modulation. The data will be used for determining if the concept will be advantageous to implement regarding performance and safety in comparison to conventional bimanual teleoperation with and without force feedback.

**Benefits and risks of participating**

During the experiment you will learn how to use teleoperation to perform unpredictable and unstructured tasks. On top of that, you will learn how to use tele-impedance to your benefit in completing the tasks.
Risks involving this experiment could be muscle fatigue due to applying force on the controller. Furthermore, dizziness of the moving environment and moving objects could occur. To counter these risks, enough resting time will be taken between experiments to relax the muscles and eyes.
Regarding the Covid-19 situation, measures will be taken to guarantee the safety for participant and researcher. First of all, the researcher will ask covid-19 related questions to evaluate if the participant is healthy. 1.5 Meter distance will be guaranteed and the participant and researcher have to disinfect their hands before the experiment starts. Furthermore, before and after the experiment, the sigma7 and table will be disinfected where the experiment takes place. If the participant or researcher notice any risk of infection or sickness during the experiment, the experiment will be stopped.

**What does participation in the research involve?**

First you will learn how to control a virtual object using the Sigma7 which is a haptic interface with seven active degrees of freedom including high-precision force-feedback. Second, you will learn how to use a circular disc interface controlled by the foot, which will add the ability to alter the stiffness of the virtual object.

After training, experiments will begin. You will perform a “drilling task” with and without force feedback having three conditions: constant high impedance, constant low impedance and variable impedance controller designs.
The drilling task consists out of two stages. First, finding the hole where you will experience force perturbations due to the rotating drill on a surface. The goal in this stage is to generate as low as possible position error to where the hole should be drilled while maintaining a constant force in drilling direction.
Second, after you have found the hole, a insertion stage will be initiated. During this stage the drill will be inserted in the hole. However, in applications the environment and robot are not ideal positioned or are moving relative to each other. Therefore, a positional perturbation is added to the environment. The goal in this stage is to generate an as low as possible force perpendicular to insertion direction and a constant force in drilling direction.
In between the experiments you will have to fill in a NASA TLX form to describe the effort you have put in to complete the tasks.

**Procedures for withdrawal from the study**

Your participation in this study is entirely voluntary and you can withdraw at any time. If you give your consent to this research, you have the freedom at all times (also during the experiment) to come back on this decision. You can request access to and rectification or erasure of personal data. You do not have to give an explanation for your decision. You can do this by contacting Stijn Klevering via s.klevering@student.tudelft.nl.

**Confidentiality of data**

This investigation requires that the following personal data are collected and used: name and surname. To safeguard and maintain confidentiality of your personal information, necessary security steps will be taken. Your data will be stored in a secure storage environment at TU Delft. Data will only be accessible to Stijn Klevering and Luka Peternel. All data will be processed confidentially and stored using a participant number only. Your name will be linked to a participant number only on the informed consent form. The informed consent form will be stored digitally in a separate and secure location and this paper form will be destroyed after digitalization. This way, all your details remain confidential. Only Stijn Klevering can know which participant number you have.

The personal data will be retained until Stijn Klevering will be graduated with the research conducted by this experiment. The data will be retained for the period the research is conducted.

The results of this study will be published in possible future scientific publications. Your participant number and name will never be shared on publications (master thesis report, scientific publications, reports) about the research.

## D.5. NASA TLX

To estimate the subjective workload of the participant, NASA TASK LOAD INDEX (TLX) was used [16]. Hart et al. 2006 reviewed 550 studies in which a NASA TLX survey was used to provide results [15]. It is common to propose and apply modified versions of the original NASA TLX scale by adding, deleting or redefining the original NASA TLX to improve relevance to target task or experimental questions. Users often point out that the subscales do significantly correlate with each other. A modification called Raw TLX eliminates the weighting process of subscales. The subscales are simply averaged to calculated the overall workload. Compared to the original version, no conclusions can be drawn due to different results about sensitivity of the survey by studies [15]. Therefore, to simplify the NASA TLX and increase time efficiency during the experiments we decided to evaluate the Raw NASA TLX illustrated on the next page.

**Figure 8.6**

## NASA Task Load Index

*Hart and Staveland's NASA Task Load Index (TLX) method assesses work load on five 7-point scales. Increments of high, medium and low estimates for each point result in 21 gradations on the scales.*

| | | |
|---|---|---|
| Name | Task | Date |

Mental Demand — How mentally demanding was the task?

Very Low — Very High

Physical Demand — How physically demanding was the task?

Very Low — Very High

Temporal Demand — How hurried or rushed was the pace of the task?

Very Low — Very High

Performance — How successful were you in accomplishing what you were asked to do?

Perfect — Failure

Effort — How hard did you have to work to accomplish your level of performance?

Very Low — Very High

Frustration — How insecure, discouraged, irritated, stressed, and annoyed wereyou?

Very Low — Very High

# E

# Experiment results

This appendix shows additional results of the effect of the circular disc interface on the drilling task regarding interaction performance with the environment during phase 1 (finding the hole task) and phase 2 (drill insertion task) and commanded stiffness ellipse accuracy. The results where statistical analyzed by an ANOVA test with Bonferroni correction. A significance level of $p \leq 0.05$ is considered as significant difference.

## E.1. Ideal stiffness ellipse strategy

We stated in appendix C the ideal stiffness ellipse strategy based on literature. The participant was instructed to use the ideal stiffness ellipse configuration to optimise their performance during the drilling task regarding position and force tracking. The ideal stiffness ellipse configuration per phase of the drilling task in illustrated in Appendix C.

For the finding the hole phase the ideal stiffness ellipse configuration is to command a high impedance perpendicular to insertion direction to increase position tracking and compensate for the force perturbation. Furthermore, a low impedance is desired parallel to insertion direction to increase force tracking for the optimal drilling reference force.

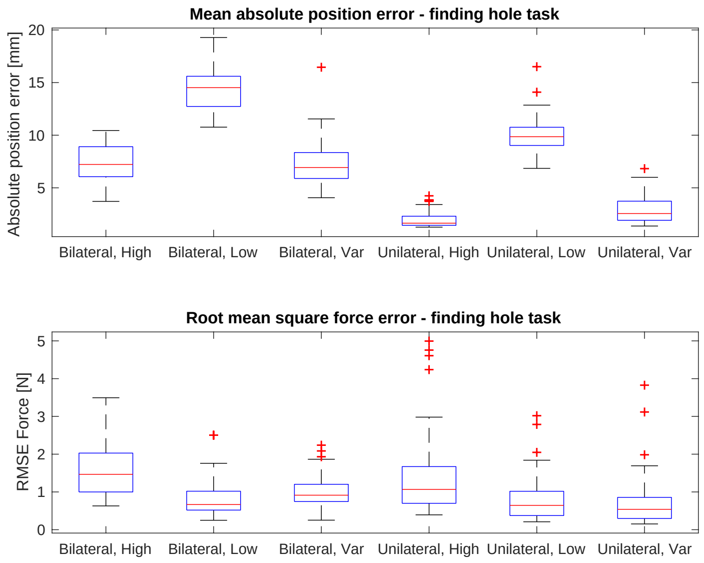

Figure E.1: The mean absolute position error during finding the hole task in the top figure and the root mean square of the force error during finding the hole task for force feedback setting and impedance control conditions.

To verify the ideal stiffness ellipse configuration we first look at the difference between high uniform impedance and low uniform impedance mode. The results are illustrated in Fig. E.1. The N-way ANOVA with Impedance mode (high uniform, low uniform and variable impedance) and force feedback settings (bilateral and unilateral) on position error perpendicular to insertion direction revealed a main effect of impedance mode and a main effect of force feedback and qualified by the interaction between impedance mode and force feedback setting as stated in the scientific paper. The position errors were lower for high uniform impedance than for low uniform impedance mode $p < .001$. Furthermore, the N-way ANOVA on force error parallel to insertion direction during the finding the hole phase revealed a main effect of impedance mode and force feedback setting but no significant interaction. The force errors were lower for low uniform impedance mode than for high uniform impedance mode $p < .001$. From these results we can conclude that the ideal stiffness configuration for the finding the hole phase presented in Fig. C.1 is the optimal stiffness ellipse configuration.

The N-way ANOVA on force error perpendicular to insertion direction during the drill insertion phase revealed a main effect of impedance mode but not for force feedback setting as stated in the scientific paper. The low uniform impedance mode indicated significant lower force errors than for high impedance mode. The N-way ANOVA on force error parallel to insertion direction during the drill insertion phase revealed a main effect of impedance mode but not for force feedback setting. Furthermore, a significant interaction between force feedback setting and impedance mode was found as stated in the scientific paper. The low uniform impedance mode indicated significant lower force errors than for high impedance mode during unilateral force feedback setting. However, for the bilateral force feedback setting no significant difference was found between high uniform impedance and low uniform impedance mode. From these results we can conclude that the ideal stiffness configuration for the drill insertion phase presented in Fig. C.1 is the optimal stiffness ellipse configuration.

Overall, the ideal stiffness ellipse configuration presented in Appendix C is accepted by the experiments. Furthermore, from the results in the scientific paper we can conclude that the ideal stiffness configuration was effective for the variable impedance mode during the drilling task.

## E.2. Stiffness ellipse semi-major axis elongation

To verify that rotational errors do not have any influence on the interaction between end effector and environment during the drill insertion phase we have to verify that the stiffness ellipse was not elongated during this phase. Fig. E.2 illustrates the elongation of the semi-major axis per phase. We can clearly see that the majority of participants did not elongate the stiffness ellipse to generate a low uniform stiffness.

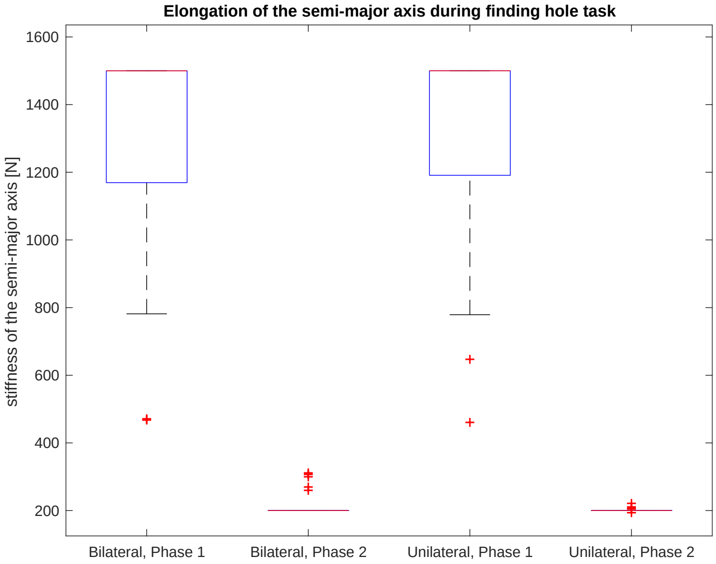

Figure E.2: The elongation of the semi-major axis per phase and force feedback setting. Phase 1 is the finding the hole phase and phase 2 is the drill insertion phase

## E.3. Rotational accuracy

The rotation of the stiffness ellipse during the finding the hole task is shown in Fig. E.3. An N-way ANOVA was conducted to compare the absolute mean rotation error between rotations of the environment and force feedback setting. However, we found no significant main effect of impedance mode F(1,109)=0.02, *p* = .896 and no significant main effect of rotation of the environment F(4,109)=1.28, *p* = .311. Consequently, we can conclude that force feedback setting does not have any influence on rotational accuracy of the circular disc interface. Furthermore, a rotation of the environment does not influence the rotational accuracy of the circular disc interface.

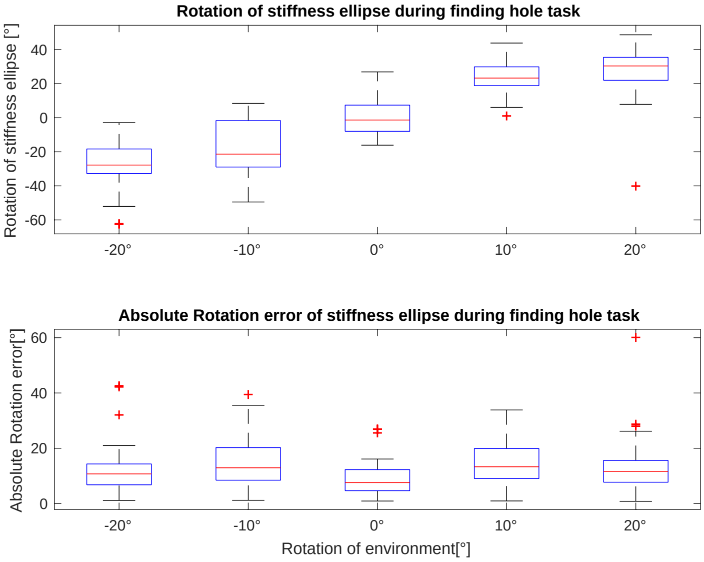

Figure E.3: Rotation of the stiffness ellipse during the finding the hole task for every rotation of the environment in the top figure and the bottom figure the absolute rotation error for every rotation of the environment

Table E.1: Overview of ANOVA results for rotational errors during variable impedance mode.[3]

| | Rotational error | | |
|---|---|---|---|
| Source | d.f. | F | p>F |
| FFB | 1 | .02 | .896 |
| ROT | 4 | 1.28 | .311 |
| FFB*ROT | 4 | .470 | .693 |
| Error | 109 | | |

[1] In the table, FFB is force feedback setting (bilateral and unilateral) and ROT are the rotations of the environment (-20, -10, 0, 10, 20 degrees). The rotational error is the error in comparison with the ideal stiffness ellipse rotation.

# Bibliography

[1] Singletact 450n force sensor. URL `https://www.singletact.com/micro-force-sensor/standard-sensors/15mm-standard-sensor/15mm-450newton/`.

[2] David A Abbink. Task instruction: The largest influence on human operator motion control dynamics. In *Second Joint EuroHaptics Conference and Symposium on Haptic Interfaces for Virtual Environment and Teleoperator Systems (WHC'07)*, pages 206–211. IEEE, 2007.

[3] A. Ajoudani, N. G. Tsagarakis, and A. Bicchi. Tele-impedance: Towards transferring human impedance regulation skills to robots. *Proceedings - IEEE International Conference on Robotics and Automation*, pages 382–388, 2012. ISSN 10504729. doi: 10.1109/ICRA.2012.6224904.

[4] Arash Ajoudani, Cheng Fang, Nikos Tsagarakis, and Antonio Bicchi. Reduced-complexity representation of the human arm active endpoint stiffness for supervisory control of remote manipulation. *The International Journal of Robotics Research*, 37(1):155–167, 2018.

[5] Panagiotis K Artemiadis, Pantelis T Katsiaris, Minas V Liarokapis, and Kostas J Kyriakopoulos. Human arm impedance: Characterization and modeling in 3d space. In *2010 IEEE/RSJ International Conference on Intelligent Robots and Systems*, pages 3103–3108. IEEE, 2010.

[6] Jacopo Buzzi, Giancarlo Ferrigno, Joost M Jansma, and Elena De Momi. On the value of estimating human arm stiffness during virtual teleoperation with robotic manipulators. *Frontiers in neuroscience*, 11:528, 2017.

[7] Jacopo Buzzi, Andrea Passoni, Giulio Mantoan, Maximiliano Mollura, and Elena De Momi. Biomimetic adaptive impedance control in physical human robot interaction. In *2018 7th IEEE International Conference on Biomedical Robotics and Biomechatronics (Biorob)*, pages 883–890. IEEE, 2018.

[8] Robert D Christ and Robert L Wernli Sr. *The ROV manual: a user guide for remotely operated vehicles.* Butterworth-Heinemann, 2013.

[9] Fredrik Dessen. Optimizing order to minimize low-pass filter lag. *Circuits, Systems, and Signal Processing*, 38(2):481–497, 2019.

[10] Luuk Maria Doornebosch, David A Abbink, and Luka Peternel. Analysis of coupling effect in human-commanded stiffness during bilateral tele-impedance. *IEEE Transactions on Robotics*, 2021.

[11] Cheng Fang, Giuseppe Rigano, Navvab Kashiri, Arash Ajoudani, Jinoh Lee, and Nikos Tsagarakis. Online joint stiffness transfer from human arm to anthropomorphic arm. In *2018 IEEE International Conference on Systems, Man, and Cybernetics (SMC)*, pages 1457–1464. IEEE, 2018.

[12] T Flash and F Mussa-Ivaldi. Human arm stiffness characteristics during the maintenance of posture. *Experimental brain research*, 82(2):315–326, 1990.

[13] THOR FOSSEN, K Pettersen, and Henk Nijmeijer. *SENSING AND CONTROL FOR AUTONOMOUS VEHICLES.* Springer, 2017.

[14] Hiroaki Gomi and Mitsuo Kawato. Human arm stiffness and equilibrium-point trajectory during multi-joint movement. *Biological cybernetics*, 76(3):163–171, 1997.

[15] Sandra G Hart. Nasa-task load index (nasa-tlx); 20 years later. In *Proceedings of the human factors and ergonomics society annual meeting*, volume 50, pages 904–908. Sage publications Sage CA: Los Angeles, CA, 2006.

[16] NASA Human Performance Research Group et al. Nasa task load index (tlx) v. 1.0: Paper and pencil package. *Moffett Field, CA: NASA Ames Research Center*, 1986.

[17] Matthew S Johannes, Robert S Armiger, Michael J Zeher, Matthew V Kozlowski, John D Bigelow, and Stuart D Harshbarger. Human capabilities projection: Dexterous robotic telemanipulation with haptic feedback. *Johns Hopkins APL Tech. Dig*, 31(4):315–324, 2013.

[18] Winfred Mugge, David A Abbink, Alfred C Schouten, Julius PA Dewald, and Frans CT Van Der Helm. A rigorous model of reflex function indicates that position and force feedback are flexibly tuned to position and force tasks. *Experimental brain research*, 200(3):325–340, 2010.

[19] Prathap Muthana, Krishna Srinivasan, Arif Ege Engin, Madhavan Swaminathan, Rao Tummala, Venkatesh Sundaram, Boyd Wiedenman, Daniel I Amey, Karl H Dietz, and Sounak Banerji. Improvements in noise suppression for i/o circuits using embedded planar capacitors. *IEEE Transactions on advanced packaging*, 31(2):234–245, 2008.

[20] Luka Peternel, Tadej Petrič, and Jan Babič. Human-in-the-loop approach for teaching robot assembly tasks using impedance control interface. *Proceedings - IEEE International Conference on Robotics and Automation*, 2015-June(June):1497–1502, 2015. ISSN 10504729. doi: 10.1109/ICRA.2015.7139387.

[21] Luka Peternel, Nikos Tsagarakis, and Arash Ajoudani. A human-robot co-manipulation approach based on human sensorimotor information. *IEEE Transactions on Neural Systems and Rehabilitation Engineering*, 25(7):811–822, 2017. ISSN 15344320. doi: 10.1109/TNSRE.2017.2694553.

[22] Satja Sivčev, Joseph Coleman, Edin Omerdić, Gerard Dooly, and Daniel Toal. Underwater manipulators: A review. *Ocean Engineering*, 163:431–450, 2018.

[23] Daniel S Walker, J Kenneth Salisbury, and Günter Niemeyer. Demonstrating the benefits of variable impedance to telerobotic task execution. In *2011 IEEE International Conference on Robotics and Automation*, pages 1348–1353. IEEE, 2011.